DEVELOPMENT AND INVESTIGATION OF AN APPARATUS FOR STANDARD PREPARATION OF ENVIRONMENTAL SAMPLES

by

YUQING TIAN, *B.Sc.*

A thesis submitted to the

Faculty of Graduate Studies and Research

in partial fulfillment of the requirements for the Degree of

Master of Science in Applied Science

Saint Mary's University

Halifax, Nova Scotia, Canada

May 1, 2006

Your file Votre référence
ISBN: 978-0-494-17654-2
Our file Notre référence
ISBN: 978-0-494-17654-2

ABSTRACT

By: Yuqing Tian

Thesis Title: Development and Investigation of an Apparatus for Standard Preparation of Environmental Samples

Date of Submission: May 1st, 2006

An apparatus for preparing particulate matter (PM) standards has been developed. Investigation and characterization of the test sample standard reference material (SRM) coal fly ash (CFA) 1633b standards prepared using this apparatus were carried out using a combination of instrumental analysis techniques. These include solution nebulization inductively coupled plasma mass spectrometry (SN-ICP-MS), laser ablation inductively coupled plasma mass spectrometry (LA-ICP-MS), and scanning electron microscopy energy dispersive X-ray spectroscopy (SEM-EDS). The results showed that homogeneous PM standards could be prepared that have potential for use in environmental monitoring of industrial emissions.

ACKNOWLEDGEMENTS

I wish to express my deepest gratitude to my supervisor Dr. Marc M. Lamoureux for opening this research opportunity to me, for teaching me the critical thinking as a scientist, and for his guidance and financial support.

I greatly appreciate Dr. David Richardson for his corrections to my thesis and his assistance in preparing for the thesis defense. I would like to thank Dr. Thomas Rand for his suggestions for the thesis writing. I would also like to thank Dr. Kathy Singfield for her time spent with me.

I wish to thank Ms Darlene Goucher and Ms. Elizabeth McLeod for their assistance with all types of technical problems. I wish to thank Dr. Xiang Yang for his assistance with using the scanning electron microscope energy dispersive X-ray spectroscopy and for his willingness to answer my questions.

I would like to thank all the people in Dr. Lamoureux's group. Ms Janelle Samson, Ms Patricia Granodos, and Ms Susan Hannan for their help with many aspects of my research.

I would also like to thank Saint Mary's University for financial support.

Finally, I would like to thank my husband Fuye Gao and my lovely son for their love and support during this endeavor.

TABLE OF CONTENTS

LIST OF TABLES

LIST OF FIGURES

LIST OF ABBREVIATIONS

PM	particulate matter
DNA	deoxyribonucleic acid
RNA	ribonucleic acid
ICP-MS	inductively coupled plasma-mass spectrometry
XRF	X-ray fluorescence spectroscopy
AAS	atomic absorption spectroscopy
INAA	instrumental neutron activation analysis
RNAA	radiochemical neutron activation analysis
PGAA	prompt gamma ray activation analysis
NDP	neutron depth profiling
OES	optical emission spectrometers
SN	solution nebulization
LA	laser ablation
DCP	direct current plasma
MIP	microwave-induced plasma
RF	radio frequency
m/z	mass-to-charge ratio
DC	direct current
UV	ultra violet
MFC	mass flow controller

PVAc	poly(vinyl acetate)
SRM	standard reference material
CFA	coal fly ash
SEM-EDS	scanning electron microscopy-energy dispersive X-ray spectroscopy
NIST	National Institute of Standards and Technology
CPS	counts per second
UPW	ultra-pure water
EPA	Environmental Protection Agency
TRA	time-resolved analysis
ppb	part per billion
RSDs	relative standard deviations
CRM	certified reference material
pg	picogram (10^{-12} g)
μm	micron or micrometer (10^{-6} m)
ng	nanogram (10^{-9} g)
nm	nanometer (10^{-9} m)
LASER	light amplification by stimulated emission of radiation
MΩ·cm	million ohm·centimeter
ms	milliseconds
L/min	litre per minute
W	Watt

M	molar (moles per litre)
MeOH	methanol
R^2	coefficient of determination
CCD	charged-coupled device
EHT	high voltage
WD	working distance
VPSE	variable pressure second electron
ANOVA	analysis of variance

Chapter 1 - Introduction

1.1 Air Pollution – Particulate Matter

Particulate matter (PM) refers to microscopic airborne particles that originate from natural and anthropogenic sources. These particles can consist of very small liquid droplets and solid particles of varying aerodynamic diameter in suspension in the air. The aerodynamic diameter (diameter, hereafter) depends on several parameters that include particle density, shape, and physical dimension. Particulate matter with a diameter of 10 μm or less (also referred to as PM10) can be found both outdoors and indoors (e.g. homes and workplaces). Particles less than 2.5 μm in diameter are referred to as PM2.5 and can penetrate deep into the lungs, thus their importance with respect to public health.[1]

Particulate matter is a mixture of materials that can include smoke, soot, dust, salt, acids, and metals. In the western United States, PM in both urban and rural areas includes major sources such as motor vehicles, wood burning stoves and fireplaces, construction sites, landfills, agriculture, wildfires and brush/waste burning, industrial sources, and windblown dust from open lands.

1.2 Metals in Airborne Particulate Matter

Heavy metals occur naturally in the environment with variations in concentration. They may be found in the earth's crust, in the atmosphere, and the hydrosphere. Metals are also released to the environment from a range of anthropogenic and natural sources. Natural sources include soil erosion due to wind, sea sprays, forest fires, and volcanic emissions. Increasing industrialization has lead to an increase in

anthropogenic sources such as fossil fuel combustion, automobile emissions, and leaching of pretreated wood. Heavy metals are usually carried on particulate matter.

The environmental and human health effects of heavy metals depend on the mobility of each metal through environmental compartments and on the pathways by which metals reach humans and the environment. The degree of concern about human and environmental health varies with each metal. Some metals are toxic; others are known to be essential micronutrients for humans and animals. However, some of those essentials for life may be toxic in excessive concentrations. Metals are among the oldest known toxin to humans;[2] for example, lead poisoning is as ancient as Roman history. Respiration and ingestion of food are two pathways by which many metals enter the human body. Metals may be directly ingested, for example by drinking water from lead pipes, or they may be indirectly ingested through bioaccumulation in the food chain (e.g. mercury in fish). Elevated concentrations of metals in airborne PM can have a serious effect on human health due to the fact that fine particulate matter (less than 2.5μm) suspended in air can penetrate deeply into the respiratory system, thus allowing the absorption of metals by the lungs.[1] Manganese, nickel, copper, zinc, and lead are among the most studied and monitored metals in airborne PM. The toxicity and sources of contamination of manganese, nickel, copper, zinc, and lead are addressed below.

1.2.1 Manganese (Mn)

Manganese is essential to normal cellular activity as a cofactor for a number of important enzymes.[3] Manganese is present in the liver, bones, and kidneys. Its metabolism is similar to that of iron. However, in excess it can cause a toxic response.[4] Excess Mn interferes with the absorption of dietary of iron. Long term exposure to excess

levels may result in iron-deficiency anemia. Increased intake of Mn impairs the activity of copper metallo-enzymes and can cause hypertension. Manganese is a known neurotoxin.

Manganese overload is generally due to industrial pollution, such as the battery manufacturing industry; manganese is also released by the steel industry. Automobile exhaust is another source of Mn pollution since an organic Mn compound is used as an anti-knocking agent in gasoline instead of lead[5]. Therefore Mn pollution occurs, along with lead, in high traffic density environments.

1.2.2 Nickel (Ni)

Nickel is a silver-white metal found in the earth's crust that is used to produce steel, Ni-cadmium batteries, heating fuel, Ni plating and ceramics. A certain amount of Ni is essential to the human body. However, too much Ni can be toxic, especially in the case of its most toxic form as Ni tetracarbonyl [$Ni(CO)_4$].[6-8] Exposure to Ni by inhalation or ingestion can increase the risk of various types of cancer, which may eventually lead to death[9]. Exposure to Ni through direct contact can cause skin rash called Ni dermatitis. Inhalation of Ni can cause asthma, nasal and sinus problems while chronic inhalation of fumes or fine particles increases the risk of respiratory cancers.[10] Nickel oxide (NiO) and Nickel subsulfide (Ni_3S_2) can pose a health hazard and are often found in PM.

In Canada, one of the most prominent sources of Ni comes from air emission released by Ni smelters. Ni is also released to the environment via wind and water erosion of soils, and volcanic eruptions.[11]

1.2.3 Copper (Cu)

Copper is an essential trace metal for life and thus required for good health. However, as with all trace metals, excess amounts of Cu in the body can be toxic. High levels of Cu are associated with physical and mental fatigue, depression and other mental problems, such as schizophrenia, learning disabilities, hyperactivity, mood swings (sometimes violent, criminal or psychotic behavior) and general behavioral problems, memory and concentration problems, postpartum depression, vascular degeneration, headaches, increased of risk of infections, sleep disorders, arthritis, spinal/muscle/joint aches and pains, hemangiomas, and several cancers.[8,12] The liver is the key organ in Cu metabolism and is the main storage site for excess Cu.[13] One of the many serious toxic effects of Cu is hepatic necrosis, which is the death of liver tissue.[12]

Copper released to land and water, thus PM, is primarily from Cu smelting industries.[14]

1.2.4 Zinc (Zn)

Zinc is less toxic than most metals.[8] Zinc is an essential trace metal for the synthesis of deoxyribonucleic acid (DNA), ribonucleic acid (RNA), proteins, insulin, and sperm. There are over 70 metalloenzymes known to require Zn for their functions.[15] However, excess Zn will interfere with the metabolism of other minerals in the body; particularly Fe and Cu. Symptoms of Zn toxicity include nausea/vomiting, fever, cough, diarrhea, fatigue, neuropathy, dehydration, and hemolysis. In addition, Zn compounds may cause chronic gastritis with excessive vomiting if they are ingested.[7]

Possible sources of Zn include: (1) galvanized pipes corroded by soft, acidic drinking water; (2) fertilizers as well as landfill leachate or industrial waste[16] and; (3) zinc smelters.

1.2.5 Lead (Pb)

Lead is a naturally occurring element that has been used almost since the beginning of civilization. Human activities have spread Pb widely throughout the environment, air, water, soil, plants, animals, and man-made constructions.[17] There is no reported health benefit associated with Pb uptake by the human body. Its presence in the body can lead to many toxic effects. Soluble ionic lead compounds can present more of a hazard than the neutral metal because it can make a way to the water system.[7] In terms of industrial exposure, the major pathways for lead to get into the body are inhalation and ingestion of Pb-bearing dust and fumes. Lead exposure typically affects the blood, nervous system, and the kidneys. The primary target areas are the brain, peripheral nervous system, kidneys, bone marrow, liver, and gastrointestinal and reproductive systems.[17] Once Pb is absorbed through the digestive or respiratory system, it binds to red blood cells and is distributed to the tissues.[4] In children, lead poisoning can cause lead encephalopathy, a disease of the brain. This may result in a loss of appetite, ataxia, coma, and death. With chronic exposure Pb may cause neurological dysfunction and inhibit hemoglobin synthesis leading to the development of anemia.[2]

Environmental Pb exposure may occur with Pb-containing paint, leaded gasoline, soil/dust near Pb industries, roadways, Pb-painted homes, plumbing leachate, and ceramic ware. Lead paint is a major source of Pb exposure for children. As Pb paint deteriorates, peels, chips, is removed, or pulverizes because of friction, house dust and

surrounding soil may become contaminated. Automobile emissions were a major source of exposure to Pb before Pb was phased out and banned as a gasoline additive. Leaded gasoline has been banned in North America since the mid 70s. Although banned in North America, leaded gasoline, in which Pb is added to gasoline as an anti-knocking agent in the form of tetraethyl lead, is still in use in other countries such as India and Mexico. Much of the Pb released to the air is deposited onto the land or surface water.

1.3 Analysis of Metals in Particulate Matter: ICP-MS

Airborne PM is a main concern regarding air pollution because it often contains heavy metals. Heavy metals in airborne PM are generally found at the trace (mg/kg) and ultra-trace (μg/kg) levels and, consequently, instrumental analysis techniques with high sensitivity for the target heavy metals are required for their analyses. A variety of techniques for elemental analysis are available, such as x-ray fluorescence spectrometry (XRF), atomic absorption spectroscopy (AAS), instrumental neutron activation analysis (INAA), radiochemical neutron activation analysis (RNAA), prompt gamma ray activation analysis (PGAA), neutron depth profiling (NDP), neutron focusing, optical emission spectrometry (OES), inductively coupled plasma (ICP)-OES, and ICP-MS. The newest of these techniques, ICP-MS, allows rapid, sequential, multi-element analysis of environmental samples.

Inductively coupled plasma-mass spectrometry was first used for elemental analysis of aqueous solutions.[18] Recognized advantages of ICP-MS include: the direct analysis of solutions; the ability to calibrate against aqueous standards; pg/mL detection limits for many elements and; both a wide elemental coverage and linear dynamic range. Although the use of aqueous solutions is usually both convenient and successful,

analytical difficulties sometimes arise. Some matrices are difficult to dissolve; therefore it is inevitable to use potentially hazardous reagents such as hydrogen peroxide (H_2O_2) and hydrogen fluoride (HF) to digest the matrix. Moreover, any sample handling involves the risk of contamination and the loss of volatile components. Also, the dissolution causes a dilution of the sample which makes the analyte detection even more difficult. In addition, dissolution procedures are laborious and time consuming. Therefore, sample preparation becomes the limiting factor in the analytical procedure of ICP-MS. Another analytical difficulty is the presence of spectroscopic and non-spectroscopic interferences in the solution sample analysis.

The operating principle of ICP-MS has not changed significantly since its introduction in 1980. An overview of the principle of ICP-MS components is given below. A more detailed description can be found elsewhere.[19-21]

1.3.1 ICP-MS: Sample Introduction System

Standard ICP-MS instrumentation uses a traditional sample introduction system comprising a peristaltic pump, a nebulizer, and a spray chamber to introduce solution. The sample is normally pumped into the nebulizer via a peristaltic pump. The benefit of a peristaltic pump is that it ensures a constant flow of liquid, irrespective of the differences in viscosity between samples, standards, and blanks. After the sample enters the nebulizer, the liquid is broken down into a fine aerosol by the pneumatic action of gas flow smashing the liquid into tiny droplets. The function of a spray chamber is primarily to allow only the small droplets to enter the ICP; the large droplets fall out and exit through the drain tube to the waste. Different types of nebulizers and spray chambers are available in the instrument market.

Real-world sample analysis requires diverse sample introduction systems. During the last 15-20 years, different sampling techniques such as, flow injection, electrothermal vaporization, and chromatography separation techniques were developed and commercialized. The modern method of solid sample (e.g. airborne particulate matter) introduction is called laser ablation (LA). In general, the process of LA includes the following steps. A laser beam is focused onto the surface of a solid sample. The laser photons are absorbed by the solid material, which leads to a rapid increase in the temperature of the sample. This subsequently leads to the vaporization of a micro amount of sample. This laser-ablated sample is now introduced into the ICP via an inert carrier gas. This method is the one used in the thesis research. Its advantages and limitations as a sample introduction method are addressed in a later section in this chapter.

1.3.2 ICP-MS: The Torch Component

Inductively coupled plasma (ICP) is by far the most common type of plasma source used in today's commercial ICP-MS and ICP-OES instrumentation. In the early days, direct current plasma (DCP) and microwave-induced plasma (MIP) were used, however, both types had some limitations. Direct current plasma instrumentation was prone to interference effects and had some usability and reliability problems. Microwave-induced plasma could reach temperatures of only 2000-3000 K, therefore it was prone to severe matrix effects and was easily extinguished during aspiration of liquid samples.[23] Inductively coupled plasma used for sample atomization and excitation of the atoms consists of an inert ionized gas (generally argon) at extremely high temperatures (6000 – 10 000 K). These high temperatures provide a suitable environment for the efficient atomization, excitation, and subsequent ionization of the sample.

The basic components for generating a plasma include a plasma torch, a radio frequency (RF) coil, and an RF power supply. Figure 1.1 shows that the plasma torch consists of three concentric quartz tubes, i.e. an outer tube, a middle tube and a sample injector. The torch is made of material (generally quartz) that is transparent to RF radiation and therefore does not weaken the field generated by the RF load-coil. Quartz can therefore withstand the high temperatures generated by the argon plasma when sufficient cooling gas (the plasma gas) is introduced into the ICP torch.

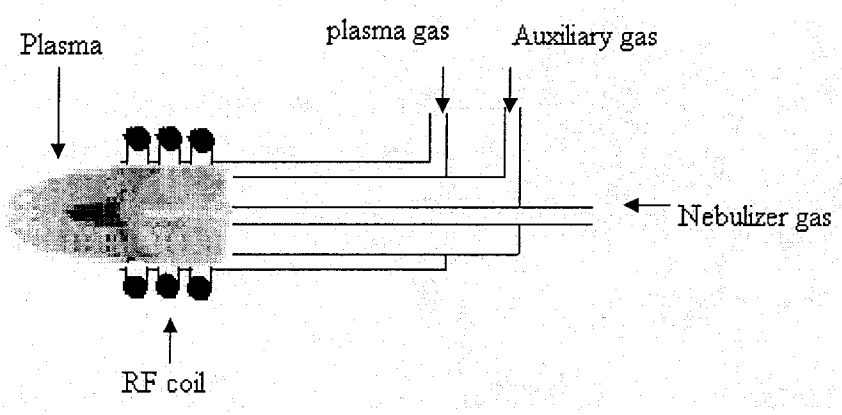

Figure 1.1 Sketch of an ICP torch showing the plasma.

The gas (usually argon) that is used to form the plasma flows between the outer and middle tubes. The auxiliary gas flows between the injector and the middle tube and is used to change the position of the base of the plasma relative to the tube and injector. The nebulizer gas, which carries the sample as a fine droplet aerosol, must have a flow rate sufficiently high to punch a channel through the center of the plasma. Although the argon is the most suitable gas for all three flows, there are analytical benefits in using other gas mixtures, especially in the nebulizer flow. For example, oxygen can be added to

the nebulizer flow gas to pyrolyze organic samples, and helium can be used in the laser ablation cell (and thus added to the nebulizer flow gas) to promote faster aerosol formation and thus minimize fractionation effects.

The plasma torch is mounted horizontally and positioned centrally in the RF coil. The load coil (usually Cu) surrounds the top end of the torch and is connected to a RF generator. When the RF power is applied to the load coil, an alternating current oscillates within the coil at a rate corresponding to the frequency of the generator. This RF oscillation of the current in the coil creates an intense electromagnetic field in the area at the top of the torch. With argon gas flowing through the torch, a high voltage spark is applied to the gas, which causes some electrons to be stripped from their argon atoms. These electrons, which are caught up and accelerated in the magnetic field, then collide with other argon atoms, stripping off more electrons. This collision-induced ionization of argon continues in a chain reaction, breading down the gas into argon atoms, argon ions, and electrons, forming an ICP discharge. The ICP discharge is then sustained within the torch and load coil as RF energy is continually transferred to it through the inductive coupling process. The sample aerosol is then introduced into the plasma through the sample injector.

The plasma discharge has different heating zones. As the sample passes through the plasma, it goes through a number of physical changes, starting at the preheating zone where the sample droplet is dried and becomes a very small solid particle, and continuing through the radiation zone where the small solid sample changes first into a gaseous form and then into ground-state atoms. Subsequently, the conversion of the atoms into ions is achieved mainly by collisions of energetic argon ions with the ground-state atom in the

analytical zone of the plasma at 6000-7000 K. The ions, representing the elemental composition of the sample, then emerge from the plasma and are directed into the interface of the mass spectrometer.

1.3.3 ICP-MS: The Interface

Although each step of a typical ICP-MS analysis – generation of a sample aerosol, sampling the representative number of analyte ions, ions transport through the interface, ion transfer via the ion optics into the mass spectrometer, detection and conversion to an electrical signal – is important, the interface is probably the most critical area of the whole ICP-MS system. The role of the interface is to transport the ions efficiently (i.e. with minimal loss), consistently, and with electrical integrity from the ICP, which is at atmospheric pressure (760 Torr), to the mass spectrometer, which typically maintains a pressure of approximately 10^{-7} Torr.

The interface is comprised of two water-cooled metallic cones of either nickel or platinum with very small orifices, which are maintained at a low pressure (ca ~ 2 Torr) by means of a mechanical roughing pump. Ions produced in the plasma pass through the first cone, the sampler cone, which has an orifice diameter of 0.8 – 1.2 mm. From there the ions travel a short distance to the skimmer cone which is sharper and has a much smaller orifice (0.4 -0.8 mm). The ions then emerge from the skimmer cone, are directed through the ion optics, and finally are guided into the mass analyzer (i.e. mass separation device). As the ion beam passes through the sampler cone into the skimmer cone, super sonic expansion of the beam will take place, but its composition and integrity will be maintained, assuming the plasma is neutral.

1.3.4 ICP-MS: Ion Optics

The role of the ion focusing system is to transport the maximum number of analyte ions from the interface region to the mass analyzer, while rejecting as many of the matrix components and non-analyte based species as possible. The ion optics are positioned between the skimmer cone and the mass analyzer, and consist of one or more electrostatically-controlled lens components. They are not traditional optics but are made up of a series of metallic plates, barrels, or cylinders that have a voltage applied to them. In addition to the main function of the ion optic system, a secondary but very important role of the ion optic system is to stop particulates, neutral species, and photons from getting through to the mass analyzer and detector. These species cause signal instability and contribute to background levels, which ultimately affect the performance of the system. Some lens systems incorporate an extraction lens after the skimmer cone to electrically pull the ions from the interface region. This has the benefit of improving the transmission and detection limits of the low mass elements, which results in a more uniform response across the full mass range.

1.3.5 ICP-MS: The Mass Analyzer

The mass analyzer is positioned between the ion optics and the detector, and is maintained under vacuum (ca $\sim 10^{-7}$ Torr). It is the heart of the ICP-MS system and it separates the ions according to their mass-to-charge ratio (*m/z*). The beam of mass-separated ions has a particular ion current, the magnitude of which is measured by a multiplier and is proportional to the population of analyte ion species in the ion beam. Therefore the magnitude of the ion current is proportional to the concentration of the analyte in the original sample.

Although various types of mass analyzers are available (including high resolution double sector ICP-MS), the quadrupole mass filter is most common and it represents approximately 90% of all ICP mass spectrometers used today.[23] A quadrupole mass analyzer consists of four cylindrical or hyperbolic metallic rods of the same length and diameter that are arranged parallel to each other. By placing a direct current (DC) field on one pair of rods and a RF field on the other pair, ions of a selected mass are allowed to pass through the rods to the detector, while the remaining *m/z* ions are rejected by the quadrupole. This scanning process is then repeated for another analyte at a completely different *m/z* until all the analytes in a multi-element analysis have been measured.

1.3.6 ICP-MS: The Detector

The detector in ICP-MS generates an electrical pulse signal (electrons) for ions of different m/z. The magnitude of the electrical pulse corresponds to the number of ions present in the sample. Therefore it is proportional to the concentration of the analyte species in the original sample. Quantitative analysis is then carried out by comparing the ion signal of an unknown sample with that of known calibration or reference standard. The most commonly used detector for ICP-MS is the discrete dynode electron multiplier.[22] The operating principle of this type detector is similar to that of a photomultiplier tube. When an ion emerges from the quadrupole, it strikes the first dynode, which then librates secondary electrons. The electro-optic design of the dynode produces acceleration of these secondary electrons to the next dynode, where they generate more electrons. This process is repeated at each dynode, generating a pulse of electrons that is finally captured by the multiplier collector or anode. The modern discrete

dynode electron multiplier uses a dual-stage discrete dynode detector to allow the determination of both high and low concentrations in one scan by measuring the ion signal as an analog signal at the midpoint dynode and as a pulse signal in the conventional way at the endpoint. The pulse-counting mode is typically linear from zero to ~10^6 counts/s, while the analog mode is suitable from 10^4 to 10^9 counts/s. To normalize both ranges, a cross calibration is required to cover concentration levels, which could generate a pulse and an analog signal. By performing a cross calibration across the mass range, a dual mode detector of this type is capable of achieving approximately eight to nine orders of dynamic range in one simultaneous scan.

1.4 Laser Ablation as a Sample Introduction Method for Particulate Matter

Inductively coupled plasma can be coupled with a variety of sample introduction devices such as solution nebulization (SN) and laser ablation (LA) technique for solid samples. Laser ablation ICP-MS was first used for solid analysis by Gray in 1985.[23]

In addition to the usual analytical advantages of ICP-MS, LA offers reduced sample preparation time, minimized contamination and dilution effects, rapid sample exchange and throughput, reduced spectral interferences (from solution), and the possibility of *in situ* spatially-resolved analysis. It is particularly attractive to scientists who want to study dissolution-resistant solid materials or study spatial distributions of trace elements and isotopic composition in a micro-scale area on sample surfaces. Therefore, LA-ICP-MS has been widely used as a powerful analytical technique for solid micro-sampling analyses in a wide variety of fields, such as geology, environmental science, biology, material science, nuclear science, and metallurgy. It is a rapid and moderate-cost analytical technique.

This technique combines the advantages of ICP-MS and *in situ* micro solid sampling of LA. It offers rapid determination of elemental concentrations of about 70 elements at a limit of detection better than 1 ng/g. Laser ablation as one type of direct analysis of solid samples is a superior introduction method because the samples are easy to prepare and some can be analyzed directly, which minimizes handling of the sample, thus decreasing the chance of contamination. Also no solvent is required, therefore no dilution effect and this reduces the formation of molecular species in the plasma that can cause spectral interferences.

However, there are some disadvantages with LA-ICP-MS. Typically, the precision and accuracy of LA-ICP-MS results are inferior to those of ICP-MS with conventional solution nebulization. One of the reasons for this poorer analytical performance is the large variation of the ablated amount owing to fluctuations in laser power, heterogeneous chemical and textural compositions, different sample surface characteristics and vaporization characteristics.[24] Elemental fractionation is a dynamic process which results in a change in relative sensitivities for certain elements between consecutive laser pulses within a single analysis. It is well known that elemental fractionation is one of the most severe limitations with the technique of LA-ICP-MS. Fractionation effects due to different ablation rates of various elements have prevented quantification without matrix-matched standards with 1064 nm Nd: YAG lasers. These effects have been reduced, but not eliminated by using shorter-wavelength ultra-violet lasers. Therefore, the optimization of the calibration process is the most significant issue associated with LA-ICP-MS.

1.5 Calibration Techniques for Laser Ablation

A variety of calibration techniques for laser ablation have been developed and applied in different fields. These calibration techniques can be divided into two classes: (1) calibration with standard solutions and (2) calibration with solid standards.[25] Calibration with standard solutions includes direct ablation[26-28] and aerosol introduction method.[29,30] Solution standards are easy to prepare. However, since the physical characteristics of solution and solid are different, so is the ablation efficiency between solution standards and solid samples. This discrepancy would generate more error for the analytical result. As a standard addition calibration technique, an ultrasonic nebulizer can be used to generate solid aerosol from standard solution. The solid aerosol and the sample vapor from the laser are transported into the ICP simultaneously. However, this standard addition method is very time consuming. Calibration with solid standards includes matrix-matched standard calibration[31-35] and non-matrix-matched standard calibration.[36]

Matrix-matched solid calibration standards with varying concentrations of analyte are ideal for LA-ICP-MS. It would permit the construction of a calibration curve by ablating standards under identical conditions as the samples. For the elemental analysis of airborne PM, samples collected on various filter media are often used. One method used to calibrate the analysis of airborne PM by LA-ICP-MS has involved the preparation of filter standards using aqueous standard solution. This would allow the standards to be introduced into the ICP via laser ablation. However, the matrix of the calibration standards is totally different from that of the actual solid samples.[37] The matrix of the standards must be closely matched to that of the samples because the ablation yield varies with the sample matrix. Another problem with this technique is that the solution

being added penetrates deep into the filter material. Therefore, in order to ensure quantitative recovery of the analyte, the sample must be ablated completely. This leads to more impurities from the filter material being transferred to the ICP-MS and consequently, the background signal from the blank can be significantly high.

Another method, which does not use solution for preparing airborne PM standards, has been developed and applied to real airborne particulate matter by Wang and Chin group.[38-40] They proposed to use a variation of a fluidized bed, which involves suspending solid standards by blowing a gas (e.g., nitrogen) at the surface of the solid powder to transport this solid suspension onto the filter. It reduced contamination from reagent solution and impurities from filter material. However, the apparatus is relatively complex. Therefore, a more simple and convenient method is desirable.

1.6 Preparation of Particulate Matter Standards for Laser Ablation Calibration

A method for the preparation of PM calibration standards onto membrane filters was recently developed in this group.[41] Fig 1.2 contains a photograph showing the PM standard preparation apparatus. This apparatus is mainly made up of two cassettes, a drift tube, and a mass flow controller (MFC). One cassette acts as a reservoir for PM, whereas the other cassette acts as a filter holder located below the PM reservoir. There is a hole in the middle of the reservoir cassette and a 5 mm height barrier around the hole. A certain amount of PM is placed in the reservoir cassette when preparing PM standards. The MFC is connected to the filter holder cassette. When the MFC is turned on, an airflow, which comes from a top cassette through a tube, suspends the PM from the reservoir cassette through the hole and the drift tube to the filter that is located in the filter holder cassette.

Another airflow, which comes from a sidearm cassette, assists to maintain the PM in suspension. A homogeneous distribution of PM on the filter is thus achieved.

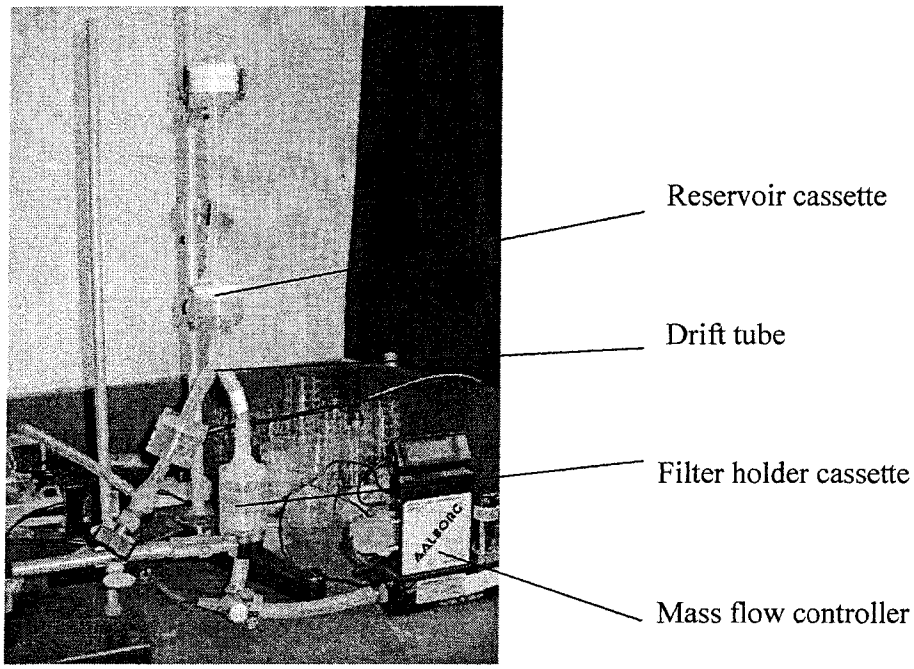

Figure 1.2 Photograph of the apparatus for preparation of PM standards (reproduced with the permission of reference 41)

To prevent the loss of PM from the filter caused by contact with other surfaces or contamination from ambient air particulate matter, a method for the application of a polymer coating was also developed to physically fix and protect the PM on the filter surface. The apparatus for polymer coating application is shown in Figure 1.3. It consists of a nitrogen tank attached to a MFC. The MFC is attached to a reagent sprayer containing the poly(vinyl acetate) (PVAc) solution. The filter to be coated is placed on a Büchner funnel attached to a suction flask. A desirable coating can be achieved by controlling the gas flow rate and application time. The polymer coating not only provides

protection to the filter and its contents, but it also aids in laser ablation. Samson[41] showed that the coating prevented excess PM around the laser ablation track from being disturbed during ablation. Figure 1.4a shows that a significant amount of PM is blown away from the LA track in the uncoated filter as compared to the coated filter in Figure 1.4b.

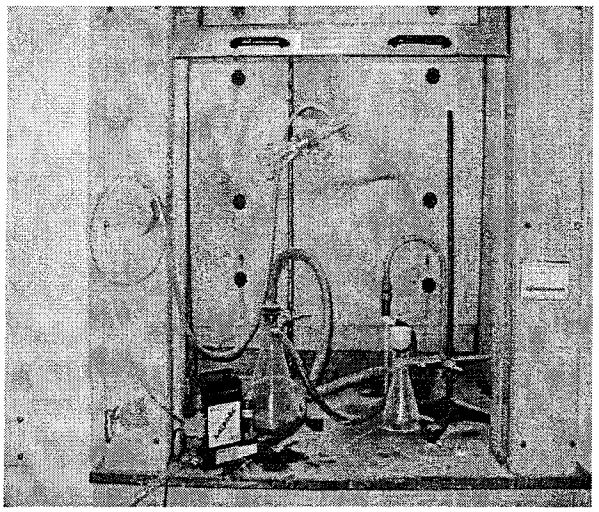

Figure 1.3 Photograph of the apparatus for PVAc coating (reproduced with the permission of reference 41)

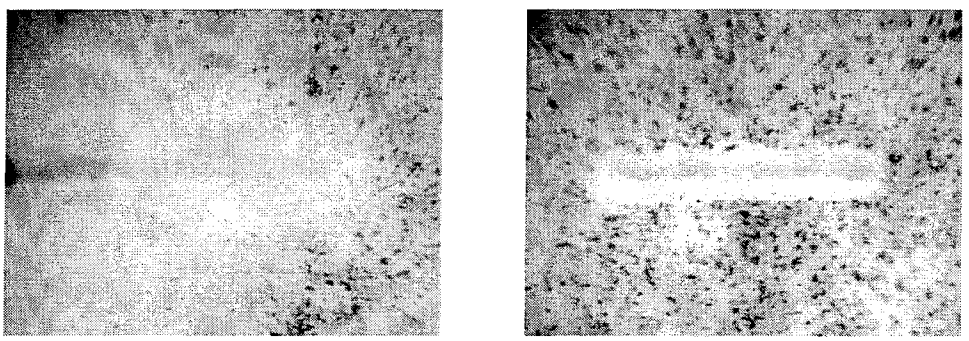

A B

Figure 1.4 CCD camera images of the (A) uncoated and (B) coated PM standard showing the laser ablation track (reproduced with the permission of reference 41)

1.7 The Present Research

The technique developed previously in our lab by Samson[41] avoided matrix effects from aqueous standard solutions and remains relatively simple and convenient. Acceptable calibration curves were generated with coefficients od determination ranging from 0.8891 to 0.9707 for standard reference material (SRM) coal fly ash (CFA) 1633b. However, the apparatus still needs improvement in order to achieve more homogeneous distribution of PM onto the filter. The general aim of this thesis research is to improve the PM distribution homogeneity on the filter which in turn will lead to an improvement in the coefficients of determination for the calibration curves of the different metals of interest in the PM sample. In order to achieve this aim, a series of objectives are put forth.

The first objective of the present study is to develop the apparatus for PM standard preparation by investigation of the impact the drift tube had on the distribution of the PM on the filter. The second objective is to investigate the chemical integrity of the test sample (SRM CFA 1633b) as a function of the physical characteristics of the reservoir cassette of the apparatus by SN-ICP-MS analysis of the acid digested sample using. The third objective is to investigate the PM standard distribution homogeneity by LA-ICP-MS and scanning electron microscopy energy dispersive X-ray spectroscopy (SEM-EDS) analysis of the PM standards. A final objective is to investigate the internal standardization method with the PVAc coating to determine its impact on the precision of the analytical results.

Chapter 2 - Development of the PM Standard Preparation Apparatus

2.1 Introduction

The PM standard preparation apparatus is mainly comprised of two cassettes and a drift tube as detailed previously in Section 1.5. Each component of the apparatus has an impact on the PM standard distribution and composition. The diameter and the length of the drift tube affect the air flow, which in turn affects the suspension and the distribution of the PM onto the filter. The configuration of the reservoir cassette influences the PM being suspended and transferred to the drift tube. The development of the components of the apparatus, the drift tube and the reservoir cassette are described in this chapter.

The chemical integrity of the PM standard prepared using the apparatus developed in this study should be the same as the original PM and therefore the certified value of the SRM could be used as standards. Acid digestion as a traditional sample preparation method was adapted for the current study. Solution nebulization ICP-MS analysis was performed, following the acid digestion, to investigate the chemical integrity of the PM standards. This was done by comparing the acid digestion recovery of the PM before and after the PM standard preparation. The acid digestion recovery of one analyte is the ratio of the concentration measured using SN-ICP-MS and the theoretical concentration calculated, based on the certificate value and the mass of the acid-digested sample. The detailed acid digestion procedure and SN-ICP-MS analysis are discribed in sections 2.4.1 and 2.4.2, respectively.

This chapter also describes the characterization of the homogeneity of the PM standards using LA-ICP-MS and SEM-EDS. The internal standardization technique with

polymer coating and helium as ablation gas were studied in order to improve the LA-ICP-MS analytical performance.

2.2 Reagents and Standards

Standard reference material (SRM) CFA 1633b [U.S. Department of Commerce, National Institute of Standards and Technology (NIST)] was used as the test PM for preparing PM standards. It should be noted that SRMs are materials for which the analytical concentration of many elements is known (A certificate of analysis accompanies each SRM). Coal fly ash 1633b has a similar matrix composition as typical urban airborne PM. This material was also used by Samson[41] and thus provides a means of comparison to assess improvements made to the PM standard preparation apparatus. The results of the analysis of PM standards using LA-ICP-MS are used to construct calibration curves which are plots of the analytical signal (counts per second) against the mass of SRM on a given filter. The calibration curves can therefore be used to determine the concentrations of elements in environmental solid samples having a matrix composition similar to the SRM standard.

The filters used in this study to prepare PM standards were EPM 2000 glass microfiber filters (Whatman International Ltd., England). The filters were pre-weighed in triplicate before and after PM transfer to determine the mass of PM on the filter using a TR-104 Balance (Denver Instrument Company, USA) with a readability 0.1 mg and repeatability ±0.1 mg. The filter standards were kept in plastic Petri dishes that were previously washed with 10% nitric acid (Reagent Grade, Fisher Scientific, Canada), and ultra pure water (UPW), with a resistivity ≥ 18.0 MΩ·cm. The UPW system is a reverse-

osmosis (Millipore, France) followed by deionized filtration system (Sybron/Barnstead, USA).

Trace metal grade nitric acid (Fisher Scientific, Canada) was used for acid digestion. 30% hydrogen peroxide (H_2O_2) (Reagent, Caledon Laboratories Ltd., Canada) was used in the acid digestion procedure for the peroxide reaction. The digestion devices used in this study were from SCP Science, which include DigiBLOC 3000 with a temperature tolerance of ± 1 °C as the heating device, 50 mL DigiTUBE (class A) as the sample container, and ribbed watch glasses for vapor recovery and reflux.

A certified drinking water sample EP-L-1 (SCP science) and a multi-element instrument check standard solution (Claritas PPT, manufactured under UL ISO 9001 Quality Assurance System) were used as the certified reference material (CRM) for SN-ICP-MS analysis.

Standard reference material 614 (trace elements in glass, U.S. Department of Commerce, NIST) was used for tuning the LA-ICP-MS operation conditions and for comparison experiments as addressed in sections 3.3.1 and 3.6, respectively.

2.3 Development of the PM Standard Preparation Apparatus

The PM standard preparation procedure described below was not changed from the previous study[41]. To transfer the PM onto the filter, the MFC needs to be opened. Thus, an airflow from a top cassette suspends the PM in the reservoir cassette, and the suspended PM is then transported through the drift tube to the filter, which is located below in the filter holder cassette in the vertical arrangement. The MFC was set to 0.5 L/min and the flow was open only to the air. Once the flow rate stabilized, the flow was opened to the apparatus and closed to the air. The flow rate was slowly raised to a desired

setting and kept open for a certain length of time. This is referred to as an "application". Once the application time was completed, the airflow was opened to the air to decrease the flow to 0.5 L/min before the next application. To add increasing amounts of PM onto the filter, the flow rate can either be increased for each application or the number of applications can be increased. It should be noted that the PM in the reservoir cassette had to be replenished after each application to keep the same mass for each application if additional applications were needed. A minimum mass of 0.25 g CFA was required as a representative sample.

2.3.1 Drift Tube Length and Diameter

The diameter and length of the drift tube between the reservoir cassette and the filter holder cassette would affect the distribution of the PM on the filter. Thus investigations were performed in which the length of the drift tube was varied while keeping the width constant at 37 mm, matching that of the reservoir cassette. Drift tube lengths used were 60, 30 and 15 cm. Visual inspection of the PM distribution was used to evaluate the effects of different length. To reduce the amount of the PM adsorbed onto the inner wall by static electricity, a hole was drilled on the top side ~5 cm from the end of the drift tube and a narrower tube which could be connected to a cassette, with a filter paper in it, was connected to the hole to allow clean air coming into the drift tube. Figure 2.1 shows the drift tube with and without sidearm. Other diameters were not studied because it was found by LA-ICP-MS and SEM-EDS analysis that homogeneous PM distribution was achieved with the 37-mm diameter.

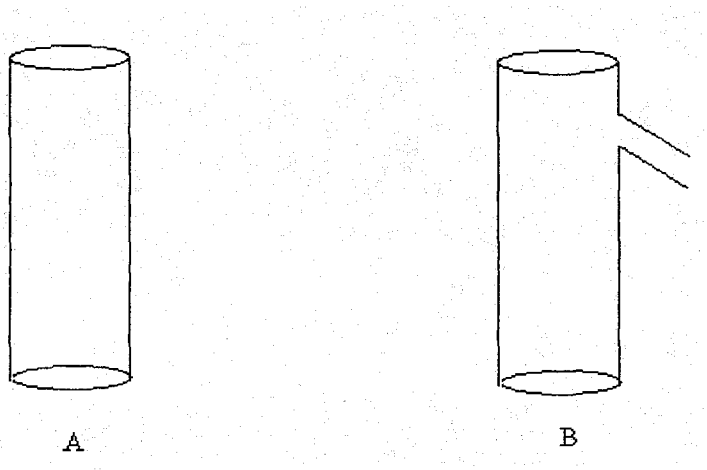

Figure 2.1 Sketch of drift tubes without (A) and with sidearm (B)

2.3.2 Reservoir Cassette

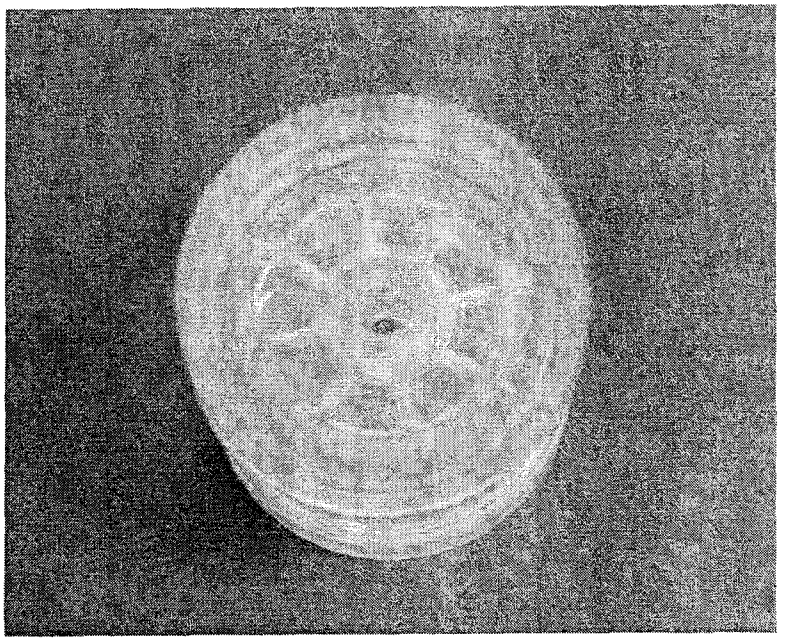

Figure 2.2 Photograph of the original reservoir cassette

A series of PM standards were prepared using the apparatus with the new drift tube and the original reservoir cassette as shown in Figure 2.2 and were analyzed by acid digestion followed by SN-ICP-MS to investigate the chemical integrity of the test sample (SRM CFA 1633b). It was found that the acid digestion recovery of the interested analytes (Mn, Ni, Cu, Zn, and Pb) in the CFA 1633b decreased after the PM standard preparation procedure. The possible reason is explained in Section 3.2.2.2. Based on that reason and the observation that some PM was accumulated around the center barrier when preparing the PM standard, it was decided that the reservoir cassette be modified as described below.

Two cassettes were glued together with their bottom sides facing each other. The two holes at the center of each cassette were connected together by a tube of correct size to form an isolated environment between the two cassettes. Figure 2.3 A shows the grooves in the reservoir cassette. Eight holes were drilled on the outer side of the grooves of the top cassette. The purpose of these holes was to permit gas to flow through from the bottom of the reservoir cassette and consequently to suspend the PM in the reservoir cassette. A thin, transparent plastic disc was also glued onto the top surface of the top cassette to provide a surface to hold the PM. This disc also had eight holes drilled into it for air flow. The film also had a same-sized hole as the center hole of the reservoir cassette to allow the PM to pass through. Two holes were drilled on the lower position of the reservoir cassette wall to connect to a compressed gas inlet. The compressed gas used in this study was nitrogen. The purpose of this gas flow was to suspend the PM from underneath. Figure 2.3 B shows the gas flow direction when the compressed gas is applied to the reservoir cassette. This configuration could allow heavier/bigger particles

in the PM to be suspended and transferred onto the filter and moreover, to reduce the accumulation of the PM around the center barrier. The final apparatus is shown as Figure 2.4.

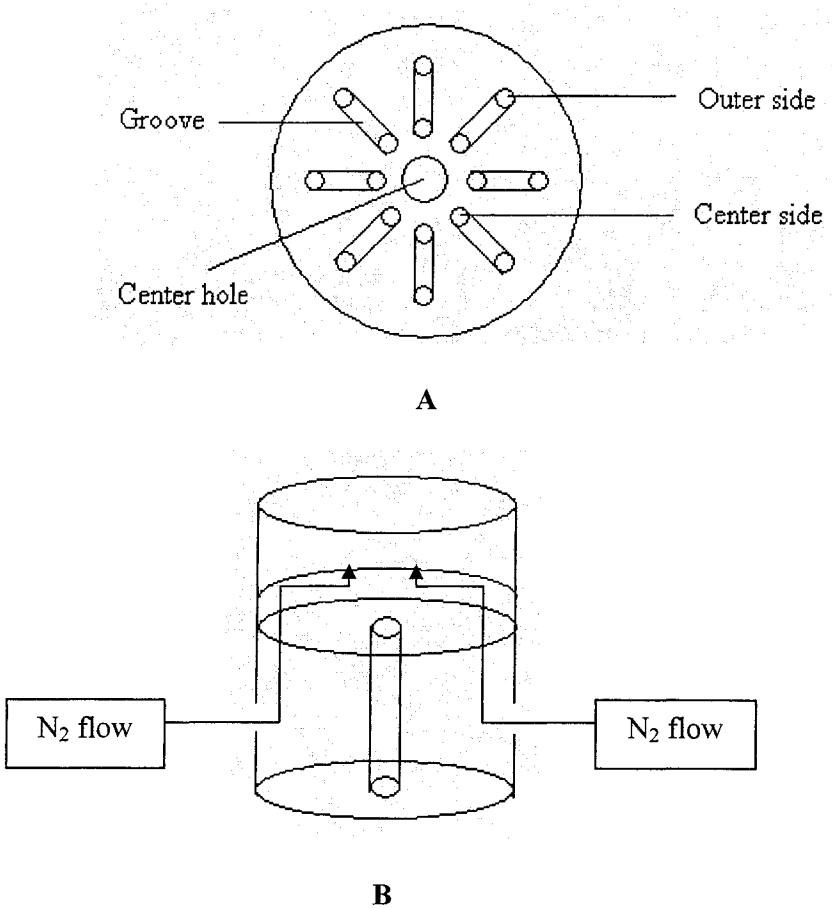

Figure 2.3 Sketch of the modified reservoir cassette (A) top view showing the grooves and (B) side view showing the N_2 flow direction.

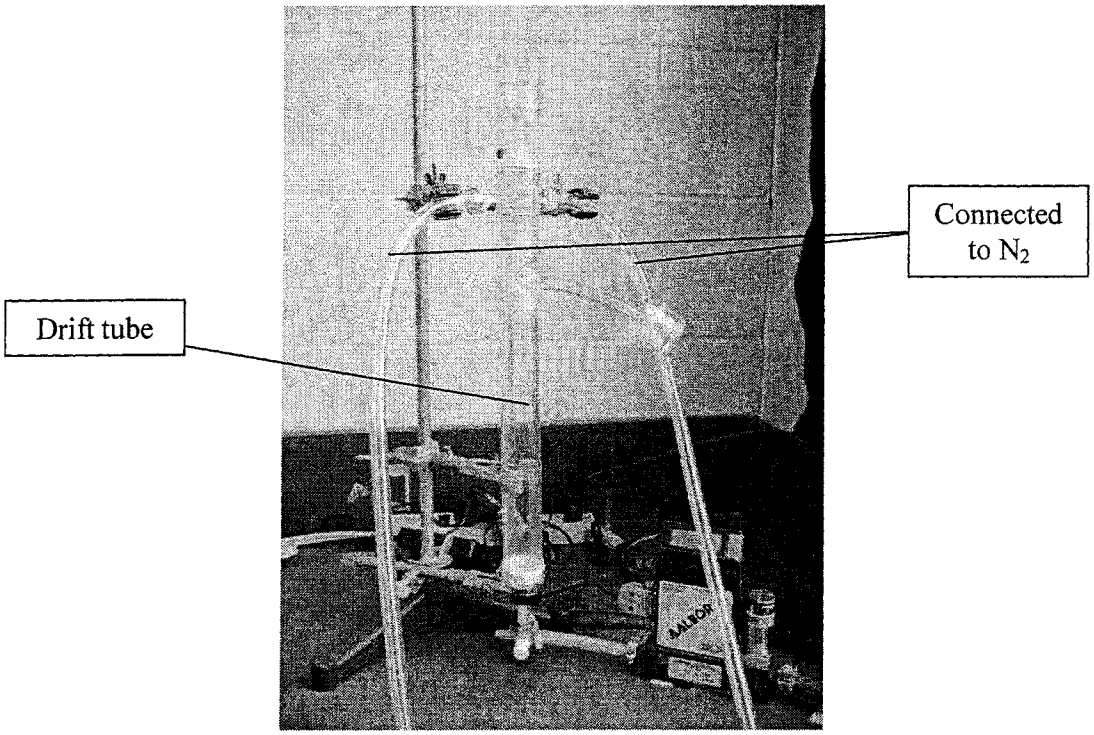

Figure 2.4 Photograph of the final apparatus for the preparation of PM standards

2.4 Chemical Integrity Investigation

The physical and chemical composition, especially the chemical composition, of the SRM that is transferred onto the filter should be maintained the same as that of the original SRM. Otherwise, the certified value of the SRM cannot be used for constructing the calibration curve and calculating the anlyte concentration of an unknown sample. Acid digestion of the SRM followed by SN-ICP-MS analysis was used to investigate the composition integrity of the SRM on the filter by comparing the acid digestion recovery of original SRM and the SRM left in the reservoir after the standard preparation.

2.4.1 Acid Digestion

The acid digestion method used in this study was based on an Environmental Protection Agency (EPA) method 3050B.[42] The flow chart is as below. It should be noted that this is an acid extractable method, not a total digestion method; therefore the recovery of the elements is expected to be <100%.

Acid digestion flow chart

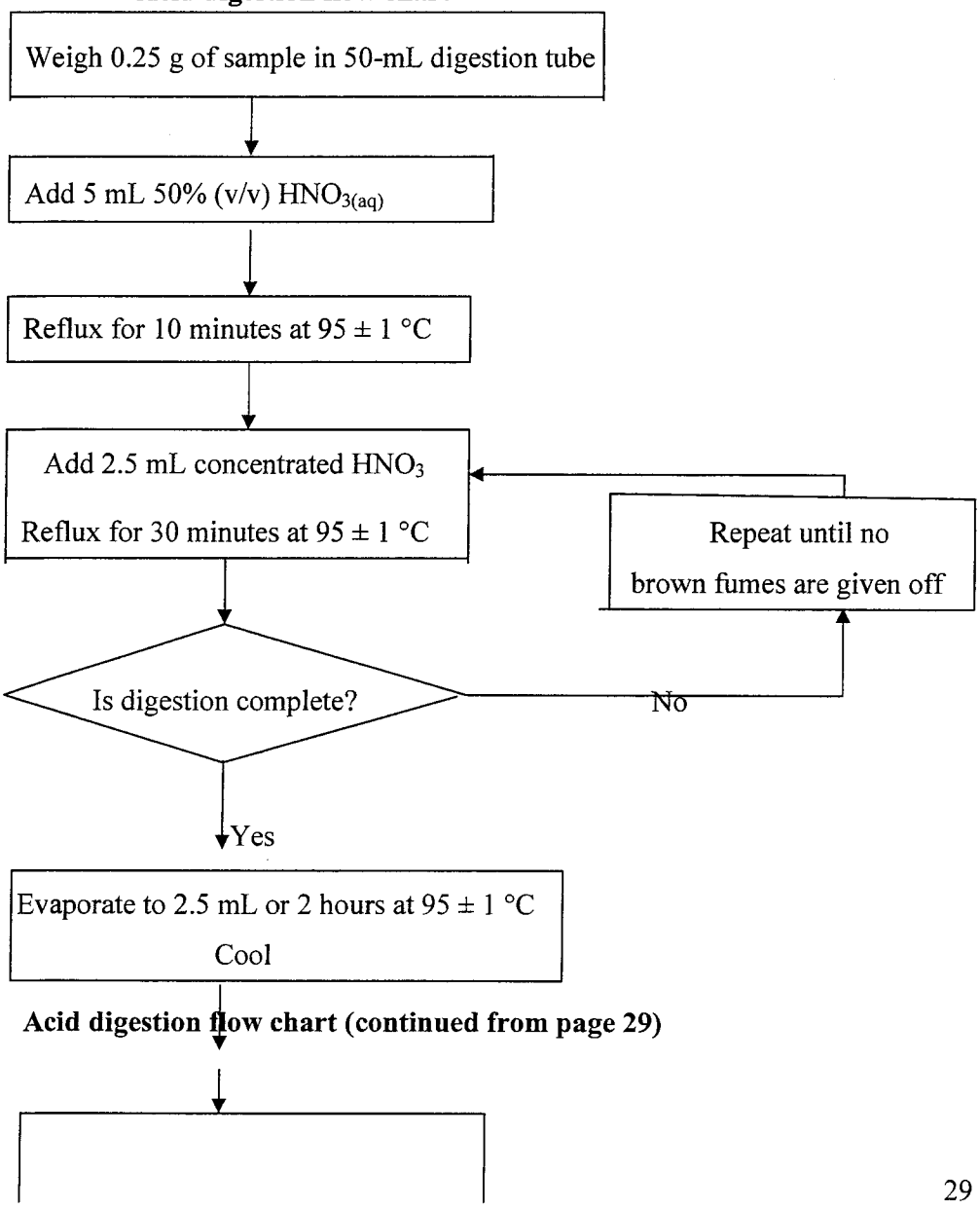

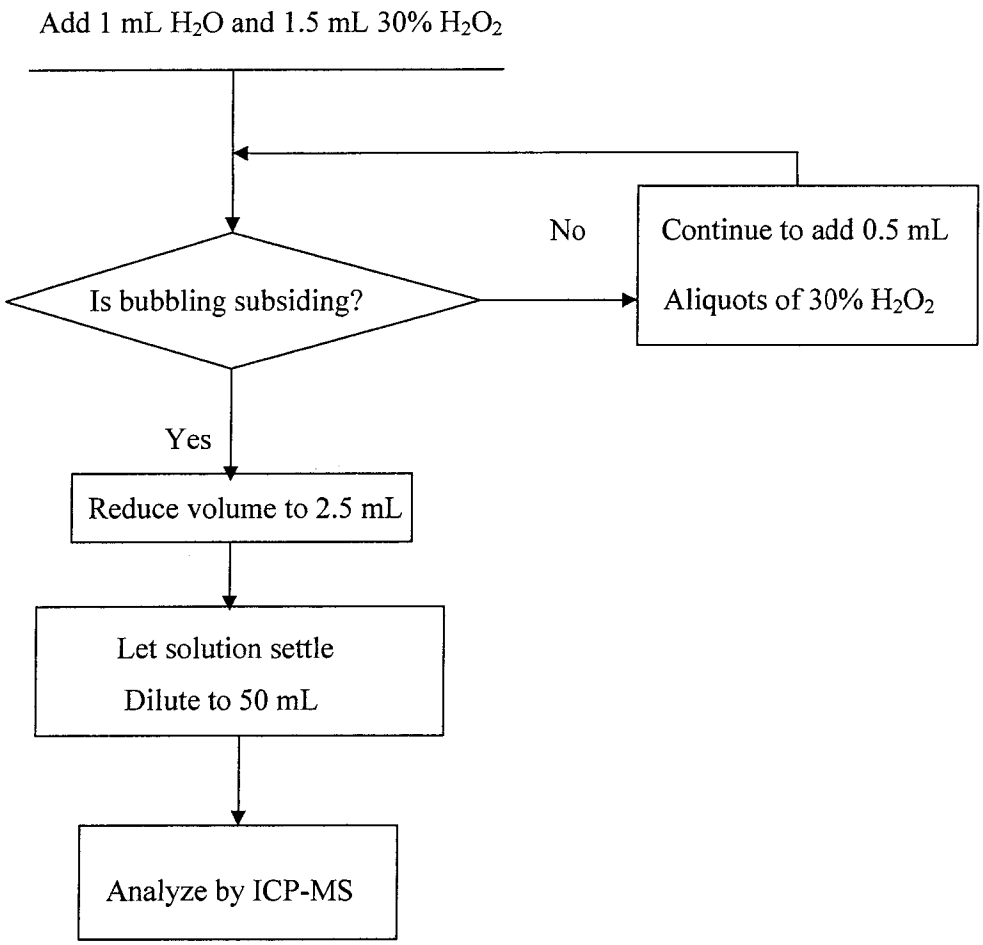

According to the requirement of the certificate of the SRM, a minimum representative sample amount of 0.25 g original CFA 1633b was used for preparing PM standards and acid digestion. The amount of PM transferred onto the PM standard ranged from 5 to 50 mg. The small amount of PM on the PM standard and the dilution effect caused by the acid digestion (as addressed in Section 1.3) can introduce large errors in the final concentration recovery result. In addition, the filter itself may contain elements that interfere with the ICP-MS analysis if the PM standard, which is prepared by applying the PM onto the filter, was digested. Therefore, the CFA 1633b left in the reservoir cassette, after the PM standard preparation, was digested and analyzed by SN-ICP-MS using the

same procedure as the original CFA 1633b for the analyte recovery comparison. The amount of CFA 1633b left in the reservoir cassette depends on the mass of CFA 1633b transferred onto the filter. When a higher mass PM standard was prepared, less mass of CFA 1633b was left in the reservoir cassette. All of the CFA 1633b left in the reservoir cassette after each PM standard preparation was collected as the sample for acid digestion and SN-ICP-MS analysis.

2.4.2 SN-ICP-MS analysis

The Thermo Elemental VG PQ Excell (Thermo Electron) ICP-MS system used in this study is a software-controlled quadrupole ICP-MS. There are three different analysis modes. The continuous mode is generally used for SN-ICP-MS. Transient time resolved analysis (TRA) is used for chromatography experiments, where the analyte peak area is proportional to the concentration of the interest. Profile TRA enables the monitoring of analyte signal changes over time. The signals can then be split up as regions of interest for reporting. The profile TRA is mainly used for laser ablation.

An auto-sampler (Cetec 500, Cetac Technologies) with a peristaltic pump (Perimax 12, Spetec) in a dustless workstation (AC600 Series, Class 100 Vertical Laminar Flow HEPA clean workstation, AirClean Systems) was used as the sampling device for SN-ICP-MS analysis.

A number of ICP-MS instrument operating conditions can be adjusted to achieve the desired analytical results. The peak-jumping mode of operation is generally selected for quantitative analysis, and peak-scanning mode for qualitative analysis. The dwell time, one parameter of MS, is the period of time that is spent on collecting data at a particular mass and usually ranges from as little as 10 ms to about 50 or even 100 ms.

Starting with the lowest mass to be analyzed, the instrument collects data for the duration of the selected dwell time and then jumps to the next mass chosen and so on. The sequence of data collected in this manner for all of the selected analyte isotopes from the lowest to the highest mass is called a sweep. In order to acquire a statistically significant amount of signal intensity data, analytical procedures usually involve several tens of sweeps. The final results for all of the data collected for a sample is usually reported as average peak intensity.

The first step for operating the ICP-MS instrument is tuning the instrument parameters to optimize the instrument operating conditions. 1 part per billion (ppb) lithium (Li), beryllium (Be), cobalt (Co), indium (In), cerium (Ce), bismuth (Bi), uranium (U) in 1% HNO_3 solution was used for tuning. The instrument signal sensitivity and stability can be optimized by adjusting the ICP parameters including the torch position; sampling depth; cool, auxiliary, and nebulizer gas flow rates; and ion optics including extraction, diffraction, three different lenses, and focus.

After tuning, a short-term stability test was performed with the tuning solution to ensure that the ICP-MS measurements are repeatable on a short-term basis. The relative standard deviations (RSDs) for all the elements in the tuning solution at less than 2% are acceptable. The standards and the unknown sample are then measured at the same conditions. A calibration curve based on a series of different concentration standards can be constructed and the analyte concentration in the unknown sample will then be determined based on the calibration curve. A 1% HNO_3 blank was used as calibration blank, 1 ppb, 5 ppb, 10 ppb, 25 ppb, and 50 ppb Mn, Ni, Cu, Zn, Pb in 1% HNO_3 solutions were used as calibration standards in SN-ICP-MS analysis. Appropriate

dilutions were made for the acid digested samples according to the sample mass and the certified analyte concentration of the CFA 1633b sample to fall in the calibration standards range. The sample list in a real analysis should include a CRM as a control sample to verify that the instrument is running properly and the analytical result is reliable. A certified drinking water sample EP-L-1 and a multi-element instrument check standard solution were used as the CRM. The instrument setting for a typical SN-ICP-MS analysis can be found in Table 2.1.

Table 2.1 ICP-MS instrumental settings for SN-ICP-MS analysis

ICP		Ion Optics	
Sampling depth	315	Extraction lens	-781
Horizontal	-70	D1 lens	-27.6
Vertical	50	Lens 1	11.0
Cooling gas flow rate	13.5 L/min	Lens 2	-67.0
Auxiliary gas flow rate	0.90 L/min	Lens 3	-70.0
Nebulizer gas flow rate	1.08 L/min	Focus	23.0
Forward power	1350 W	Pole bias	2.0

2.5 The PM Standard Homogeneity Investigation

Once the chemical integrity of the SRM of the PM standard was established, the SRM should also be homogeneously distributed to ensure that the PM standard is reliable, thus the certified value could be used to establish the relation between the signal and analyte concentration. Homogeneity is also related to the coefficient of determination (R^2) of a calibration curve of a series of standards. A R^2 value close to 1.0000 indicates that good sample homogeneity on the filter. Laser ablation ICP-MS analysis was performed to investigate the homogeneity of the trace elements Mn, Ni, Cu, Zn, and Pb. Scanning

electron microscope (SEM) attached to energy dispersive X-ray spectroscopy (EDS) was used to investigate the homogeneity of the major elements Al, Ca, Fe, Mg, K, Si, Na, S, and Ti.

2.5.1 LA-ICP-MS Analysis

The LA unit (Microprobe II-266 LUV 266X Laser Ablation System, New Wave Research Merchantek Products, USA), which is used as a solid sample introduction device for ICP-MS in this study, operates at UV wavelength 266 nm. The 266 nm Nd: YAG laser is the most widely used source for LA-ICP-MS. It is reliable, easy to use, relatively cheap, and is sufficiently highly absorbed for controlled ablation of most minerals[43]. Comparisons between different wavelengths indicated that UV wavelength has better absorption and detection limits and less elemental fractionation, which is one of the most severe limitations with the technique of LA-ICP-MS.[43,44] As mentioned in 2.4.2, profile TRA was used as data acquisition mode. Once the analytes and timeslices have been defined data can be acquired for post-acquisition processing.

Standard reference material NIST 614 was used for tuning the ICP parameters and ion optics of MS under certain laser conditions, the instrument signal were optimized to achieve the highest sensitivity. It has been pointed out by Samson[41] that the use of a polymer coating on the filter's surface has not only the advantages of protecting the contents of the PM standard and aiding in laser ablation track, but it also allows the use of the internal standardization technique. All the PM filter standards analyzed by LA-ICP-MS were coated with PVAc, which is described in detail at section 2.5.1.1. It also should be noted that helium was used as the ablation cell gas during LA-ICP-MS analysis because of its advantages as discussed at section 2.5.1.2.

Seven raster patterns were ablated on a coated 9.37 mg PM standard (Figure2.5) by the laser ablation unit and measured by the ICP-MS. The homogeneity of the trace elements Mn, Ni, Cu, Zn, and Pb in the PM 1633b on the filter was evaluated by comparing the integrated element transit signal of the seven different rasters. The RSDs, a statistical parameter, were calculated to evaluate the homogeneity of the PM standard.

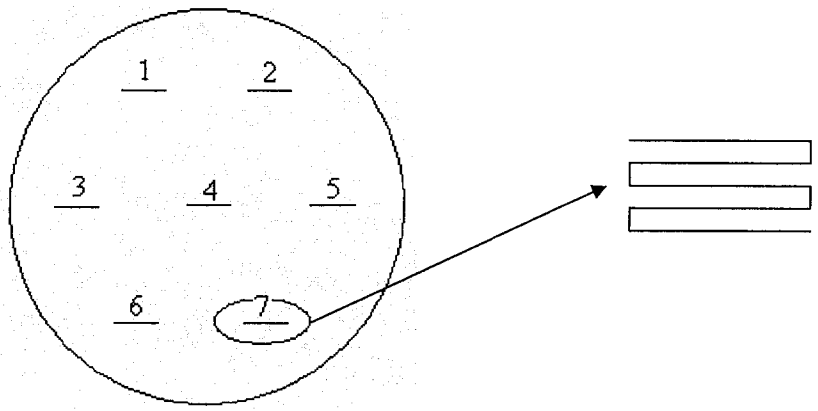

Figure 2.5 Sketch showing the placement of the seven sites of laser ablation on the PM standard, showing raster pattern.

A small portion of filter with PM was cut from each standard of a series of PM standards and arranged on a glass slide using double-sided tape and analyzed by LA-ICP-MS to construct a calibration curve and thus establish the relationship between the analytical signal and sample concentration and evaluate the homogeneity of the PM standard. For analysis, the laser was pulsed at 10 Hz with 40.0% output. The laser output was chosen so as to ablate completely through the PM on the filter but not the filter. Three raster patterns on each PM standard were ablated by laser and measured by ICP-MS. The average of the three signals was used for constructing the calibration curve. The

instrument settings were as Table 2.2 for LA and Table 2.3 for ICP-MS. Calibration curves were prepared using the least square regression method.

Table 2.2 Laser settings

Raster spacing	Scan speed	Depth/pass	Output	Repetition rate	Spot size
150.0 μm	60 μm/s	10 μm	40.0%	10 Hz	50 μm

Table 2.3 ICP-MS instrumental settings for LA-ICP-MS analysis

ICP		Ion Optics	
Sampling depth	345	Extraction lens	-707
Horizontal	26	D1 lens	-35.1
Vertical	117	Lens 1	-0.4
Cooling gas flow rate	13.0 L/min	Lens 2	-60.5
Auxiliary gas flow rate	0.90 L/min	Lens 3	-50.6
Nebulizer gas flow rate	1.15 L/min	Focus	11.5
Forward power	1350 W	Pole bias	-4

2.5.1.1 PVAc Coating with Internal Standards

A solution of 0.01M PVAc in methanol (MeOH) is used with a sprayer to form a fine mist which is deposited on the surface of the PM standard to act as a protective coating. This method was already used successfully by Samson[41]. No changes were made regarding the polymer coating apparatus and its operation. The set-up is shown in Figure 1.3. In order to spray the PVAc solution onto the PM standard, the nitrogen tank is open and the flow rate is set at 2.5 L/min, thus a fine mist of PVAc solution is generated. The

position of the sprayer is adjusted to obtain a homogeneous distribution of PVAc coating on the Büchner funnel. The PM standard is placed in the Büchner funnel and covered with a piece of hard paper on the top of the funnel. Once the nitrogen flow is stable and the sprayer position is adjusted, the hard paper is removed thus the PM standard is open to the PVAc fine mist and applies the coating for two minutes.

The use of the internal standardization calibration technique can correct the variation in the ICP-MS signal caused by sample matrix and/or instrument drift, thus improving both analytical accuracy and precision. Therefore, 1 ppb internal standards beryllium (Be), indium (^{115}In), and bismuth (^{209}Bi) were added into the solution when preparing the PVAc solution and applied onto the PM standards during the coating procedure. ICP-MS would acquire the signal for both analytes and internal standards at the same run. The analyte signal can then be normalized to the internal standards to minimize the signal variation due to the instrument drift or sample matrix effect.

2.5.1.2 Helium as Ablation Gas

Elemental fractionation, one of the most severe limitations with the technique of LA-ICP-MS, can generally be recognized on time-resolved intensity plots as a non-correlation of signals for different elements. This phenomenon has been reported to occur with all types of lasers and studies have compared fractionation produced at different wavelength LA systems, but meaningful comparisons between wavelengths are always extremely difficult because wavelength is not the only critical parameter influencing elemental fractionation. Other operating conditions such as beam homogeneity, power density, pulse width, focus position, carrier gas also affect elemental fractionation.[45-47] The ablation gas used (Ar or He) can have a significant effect on fractionation

characteristics. Eggins *et al.*[48] and Günther and Heinrich[45] indicated that helium argon mixture as carrier gas, yields a 2 - 3-fold sensitivity enhancement and greatly reduced background intensity. The increased signal intensities are mainly due to the greatly reduced surface deposition by ablating in an ambient atmosphere of He and improved particle transport from the ablation cell into the ICP-MS. Whereas Guillong and Günther[49] indicated that using 193 nm laser, a 3-fold increase in signal intensity is achieved in helium as a result of a 2.5-fold increase in sample transport. However, using a 266 nm laser did not show such an intensity enhancement. These works suggested that the presence of helium gas in the ablation cell provides a beneficial effect relative to argon, e.g. on particle size distribution, aerosol transport, and reduced elemental fractionation.

In this study, because of its benefit as an ablation/carrier gas, helium was connected to the laser ablation unit instead of the previous used Ar. The comparison between the Ar gas and He gas as the ablation gas was done with the NIST SRM 614. The configuration of the He connection is shown in Figure 2.6.

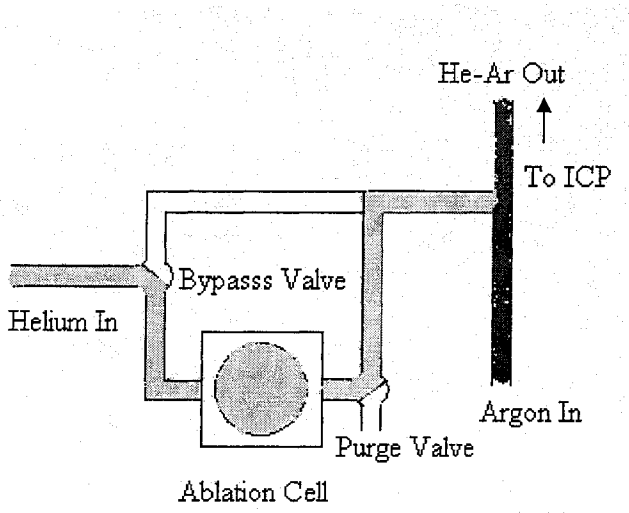

Figure 2.6 Diagram showing the helium-argon gas flow.

2.5.2 Scanning electron microscope-energy dispersive X-ray spectroscopy (SEM-EDS) analysis

The scanning electron microscope-energy dispersive X-ray spectroscopy instrument used in this study is LEO 1450 VP SEM attached Oxford INCA 200 EDS. Energy dispersive X-ray spectroscopy identifies the elemental composition of materials imaged in a SEM. As the electron beam of the SEM is scanned across the sample surface, it generates X-ray fluorescence from the atoms in its path. The energy of each X-ray photon is characteristic of the element which produced it. The EDS microanalysis system collects the X-rays, sorts and plots them by energy, automatically identifies and labels the elements responsible for the peaks in this energy distribution as a spectrum. Figure 2.7 is an example of EDS spectrum of a PM (CFA 1633b) standard.

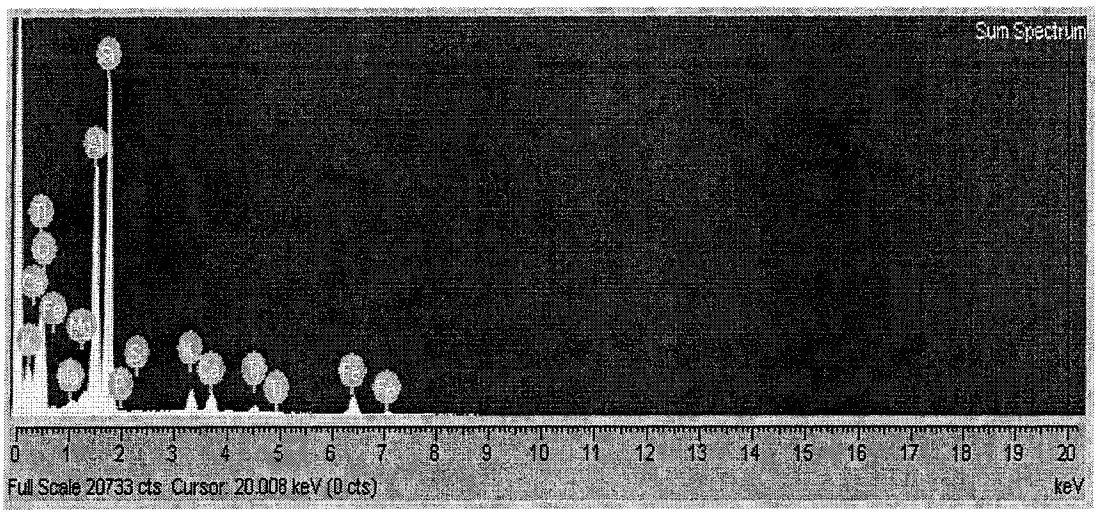

Figure 2.7 An EDS spectrum of a PM standard showing elemental X-ray emission energy intensity as a function of energy.

The EDS is a common attachment to the SEM and provides the capability of simultaneous elemental distribution maps, thus giving a visual representation of the

chemical distribution in the sample. When the EDS data are compared with either known or computer-generated standards, a full quantitative analysis showing the sample composition can be produced. Most elements are detected at concentrations of order 0.1%. Therefore EDS attached SEM was used to investigate the homogeneity of the PM standard in present study as a substitute of LA-ICP-MS for major elements Al, Ca, Fe, Mg, K, Si, Na, S, and Ti. Seven images were made and measured on a 10.07 mg and a 21.28mg PM standards (Figure 2.8). The instrument settings can be found in Table 2.4.

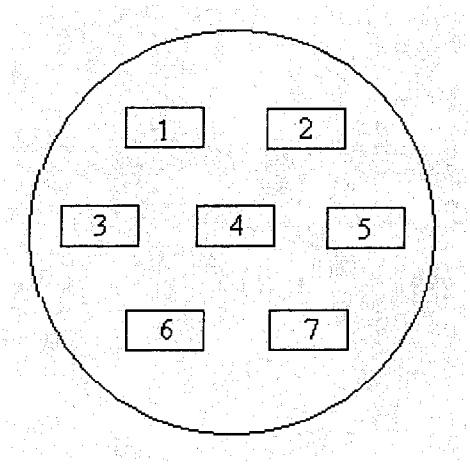

Figure 2.8 Sketch of the PM standard showing the areas selected for SEM-EDS analysis.

Table 2.4 EDS settings for a 21.28mg PM standard analysis

EHT	20.00 kV
WD	20 mm
VPSE	4.4×10^{-1} Torr

Chapter 3 - Characterization of the PM Standard Preparation Apparatus

3.1 Introduction

The impact of the length and diameter of the drift tube of the apparatus on the distribution of PM on the filter was evaluated by visual inspection and LA-ICP-MS analysis. The coefficient of determination, which ranged from 0.9622 for Zn to 0.9819 for Mn, was significantly improved compared with previous values which ranged from 0.8891 to 0.9707. [41]

The chemical integrity of the test sample SRM CFA 1633b, as a function of the physical characteristics of the apparatus, was investigated by analyzing the acid digested sample using SN-ICP-MS. The acid digestion procedure was investigated in a preliminary way using the NIST original SRM CFA 1633b and then used to investigate the chemical integrity of the PM SRM CFA 1633b standards. The SN-ICP-MS data, which were analyzed using the statistical data treatment and evaluation technique, supported the hypothesis that the PM standard preparation procedure did not change the chemical composition of the original SRM CFA 1633b.

Statistical tests are the tools scientist use to sharpen their judgment concerning the quality of experimental measurements. The *t*-test is usually used for comparison of two experimental normally distributed data. However, the normal *t*-test requires that the standard deviations of the data sets being compared are equal. The F-test, another simple statistical test, can be used to test this assumption under the provision that the populations

follow a normal (Gaussian) distribution. The F test is also used for comparing more than two means. The methods used for multiple comparisons fall under the general category of analysis of variance (ANOVA),[50] which is one of the most common applications of statistical tests. The single factor ANOVA method uses a single test to determine whether or not there is a difference among the population means rather than pair-wise comparisons, as are done with the *t*-test. If ANOVA indicates a potential difference, multiple comparison procedures can be used to identify which specific population means differ from others. If the calculated F value is smaller when compared with the critical F value at a significance level of α, the population means are statistically identical. Thus the numerical difference is the result of random error, which is inevitable in all measurements, or it is the result of systematic error.

Three population means, (i) the acid digestion recovery of the original CFA 1633b; (ii) the recovery of the CFA 1633b left in the reservoir after the first series of standards preparation procedure; and (iii) the recovery of the CFA 1633b left in the reservoir after the second series of standards preparation procedure, were compared at a significance level of 0.05 using ANOVA in this study. Analysis of variance technique was also employed in the investigation of the acid digestion method.

Particulate matter standard homogeneity was investigated using a combination of instrument analysis techniques of LA-ICP-MS and SEM-EDS by analyzing seven representative areas of one PM standard. Relative standard deviation (RSD), a statistical parameter, was used to evaluate the results. The RSD of seven raster LA-ICP-MS transient signal intensity was comparable with a homogeneous SRM NIST 614. A better coefficient of determniation was obtained with a series of six PM standards analyzed by

LA-ICP-MS. Both LA-ICP-MS results provided the evidence of that the PM standards prepared using the apparatus developed in this study were homogeneous. The SEM-EDS results also provided evidence for homogeneously distributed PM on the filter.

The preliminary investigation of internal standardization technique associated with polymer coating, and the effect of helium on LA-ICP-MS signal as ablation gas, were reported in this chapter. The effect of PVAc coating on the signal is also discussed.

3.2 The Investigation of the PM Standard Preparation Apparatus

3.2.1 The Drift Tube

Based on the existing apparatus as described in Chapter 1, the performance of the drift tubes at different lengths (60 cm, 30 cm, and 15 cm) were investigated. A longer drift tube could offer more time for the PM suspension and result in a more homogeneous PM distribution on the filter from the theoretical viewpoint. However, a longer tube also increases the chance of the PM being adsorbed onto the inner wall of the drift tube which was not expected. No PM distribution difference on the filter was found for different length drift tubes by visual inspection. Therefore a 30-cm long tube was chosen as the drift tube. The investigation in 3.3 showed that homogeneously distributed PM standards could be obtained with the 30-cm drift tube. Figure 3.1 contains a photograph of a CFA 1633b standard prepared using the apparatus with the 30 cm drift tube.

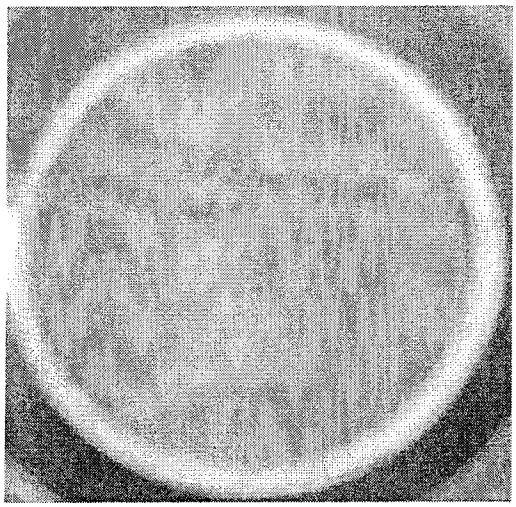

Figure 3.1 A photograph of a 12.19 mg PM standard

Since some PM was adsorbed onto the inner wall of the drift tube during the PM standard preparation process, a hole was drilled into the tube to connect a sidearm to allow some air to flow in a spiral fashion inside the drift tube (Figure 2.1). It was found, by visual inspection, that the sidearm on the tube was useful for reducing the amount of PM adsorbed onto the inner wall of the drift tube while maintaining a homogeneous distribution of PM on the filter. With the sidearm on, the total airflow passing through the mass flow controller generated by the vacuum pump was split into two flows. One flow, from the top of the reservoir cassette, suspended the PM placed in the reservoir cassette. The other flow passed through the sidearm to assist the PM suspension in the drift tube. Therefore, a double airflow rate was needed to transfer a similar amount of PM onto the filter. However, higher flow rates would deposit the PM onto the filter more compactly.

3.2.2 The Reservoir Cassette

The reservoir cassette was modified according to the chemical composition of the PM (SRM CFA 1633b) before and after the PM standard preparation procedure. The chemical composition of the test sample SRM CFA 1633b was investigated by analyzing the acid digested sample using SN-ICP-MS.

3.2.2.1 Acid Digestion

The acid digestion method (as detailed by the flow chart in Section 2.4.1) is based on EPA 3050B. This method is not a total digestion technique. It is a very strong acid digestion that will dissolve almost all elements that could become "environmentally available". In this procedure, one step was difficult to achieve, specifically the instruction to add 2.5 mL concentrated nitric acid until no brown fumes are given off was difficult to execute. The depletion of the fumes indicates a completed reaction. However, it was found that brown fumes were always given off, even for the blank. Therefore different amounts of concentrated nitric acid were investigated in order to determine the most suitable amount of acid needed for the complete acid digestion. The details of these experiments are listed in Tables 3.1 through 3.3. The results were analyzed using ANOVA and indicated that increasing the volume of concentrated HNO_3 did not increase the acid digestion recovery; rather, the details of the ANOVA F values showed that statistically identical recoveries were obtained for different volume of concentrated HNO_3. In addition, longer sample reflux and evaporation times would be needed if more acid were used to digest the sample. This could cause digestion tube breakage. Therefore, 10 mL HNO_3 was determined as the most suitable amount of acid needed for the acid digestion.

It should be noted that the Ni recovery is not available because of the isotope ^{58}Ni selected for the ICP-MS measurement. Iron (Fe) isotope at mass 58, which is present in CFA 1633b at even higher concentration than Ni, interfered with the Ni analysis and it could not be corrected for by calculation because Fe was not measured during the analysis. This problem was realized when doing the recovery data analysis after the experiment which was not repeated. Therefore the measured Ni recovery, which includes ^{58}Fe, is inaccurate. However, a conclusion still can be drawn that 10 mL concentrated HNO_3 is sufficient for the acid digestion process. The reservoir cassette configuration was developed based on this acid digestion method.

Table 3.1 A list of CFA 1633b acid digestion recovery % (10 mL HNO_3)

Mass (g)	Mn	Ni	Cu	Zn	Pb
0.2522	35.7	na	33.4	35.2	41.7
0.2520	35.3	na	32.9	35.1	41.5
0.2532	38.0	na	33.2	43.9	41.7

Table 3.2 A list of CFA 1633b acid digestion recovery % (15 mL HNO_3)

Mass (g)	Mn	Ni	Cu	Zn	Pb
0.2540	34.3	na	31.0	32.7	39.3
0.2511	35.8	na	32.1	34.2	41.1

Table 3.3 A list of CFA 1633b acid digestion recovery % (20 mL HNO_3)

Mass (g)	Mn	Ni	Cu	Zn	Pb
0.2472	39.6	na	34.5	37.3	43.4
0.2495	37.6	na	35.0	36.2	40.9
0.2500	37.1	na	32.7	34.5	39.5

3.2.2.2 Development of The Reservoir Cassette

Aseries of filter standards was prepared using the apparatus with the original reservoir cassette (Figure 2.2) using test sample CFA 1633b. The CFA 1633b left in the reservoir cassette was digested using the acid digestion method described in section 3.2.2.1 and analyzed by SN-ICP-MS. The results are listed in Table 3.4. Two original SRM CFA 1633b samples were also analyzed at the same time. It can be seen that the acid digestion recovery decreased when the mass of CFA 1633b left in the reservoir cassette decreased. Such as Cu recovery decreased from 42% to 31% roughly, and Pb recovery decreased from approximately 45% to 24%.

Table 3.4 Acid digestion recovery (%) of SRM CFA 1633b left in the reservoir cassette after PM standard preparation with the original reservoir cassette

Mass (mg)		Mn	Ni	Cu	Zn	Pb
Original CFA 1633b	250.26	38.53	34.71	42.72	45.89	46.34
	252.89	38.70	32.79	41.96	45.99	44.99
CFA 1633b left in the reservoir cassette after standard preparation	202.90	40.10	34.93	41.01	43.61	40.32
	199.42	39.79	33.00	38.63	40.08	39.41
	179.83	38.93	33.90	38.65	39.93	42.52
	121.27	38.21	30.12	33.29	33.52	24.60
	114.69	40.54	28.62	31.32	29.01	26.14
	109.15	38.39	29.97	30.79	28.06	24.18

There was no chemical process occurring during the PM standard preparation procedure, and therefore it is assumed that the change in the acid digestion recovery of CFA 1633b is due to changes in the physical composition of the CFA 1633b before and

after the PM standard preparation. That is, the more indigestible (probably bigger/heavier) particulates were left behind in the reservoir cassette and the easily digestible (probably smaller/lighter) particulates were transferred onto the filter when preparing the PM standard. Therefore the fraction of digestible particulates left in the reservoir cassette was smaller resulting in the decreased acid digestion recovery. A phenomenon was observed that some PM tended to accumulate around the barrier of the reservoir cassette center hole was observed during the PM standard preparation. The reservoir cassette was modified as described in Section 2.3.2 based on this assumption and the phenomenon observed.

Two series of nine and twenty PM standards were prepared using the modified reservoir cassette with nitrogen gas blowing from underneath at a flow rate of ~ 8 L/min. The CFAs left in the reservoir cassette were digested and analyzed by SN-ICP-MS. The results are shown in Table 3.6 and Table 3.7. Table 3.5 is the acid digestion recovery of original CFA 1633b. Statistically identical recoveries as shown in Appendix 2 for the whole mass range of CFAs were obtained with the original CFA 1633b except for Ni. The recoveries of Ni for the first series of nine samples were different from the original sample. This could be caused by the fact that the sample cone of the ICP-MS was made of Ni, which affects the accuracy of Ni analysis especially when it was worn. However, the recoveries of Ni for the second series with larger sample size of twenty samples were the same as for the original CFA 1633b as shown in appendix 2. The same acid digestion recovery, of the SRM CFA 1633b left in the reservoir cassette after the PM standard preparation, with the original one, indicated that the chemical integrity of the CFA remained after the PM standard preparation.

Table 3.5 Acid digestion recovery (%) of original CFA 1633b

Mass (mg)	Mn	Ni	Cu	Zn	Pb
250.26	38.53	34.71	42.72	45.89	46.34
252.89	38.70	32.79	41.96	45.99	44.99
252.13	37.37	32.19	41.06	38.73	40.94
256.03	37.81	31.38	38.91	37.36	40.09
254.72	38.44	31.56	39.75	42.10	42.52
251.10	36.07	30.47	38.66	40.82	41.88
254.20	37.21	33.31	40.81	46.23	42.20
252.77	39.40	33.60	41.92	45.17	44.30

Table 3.6 Acid digestion recovery (%) of CFA 1633b left in reservoir cassette after PM standard preparation with the modified reservoir cassette (9 samples)

Mass (mg)	Mn	Ni	Cu	Zn	Pb
204.43	36.99	29.69	37.16	38.76	40.22
197.75	36.32	29.46	39.54	44.39	39.20
189.72	38.26	30.16	38.32	40.99	40.47
185.37	40.65	29.37	36.99	38.55	38.55
181.50	37.88	30.64	38.24	38.06	40.73
167.37	37.43	29.26	39.04	39.36	39.38
158.21	38.44	31.90	38.94	41.62	42.14
154.30	37.89	30.39	44.53	42.75	45.52
100.08	40.53	31.76	37.35	37.63	46.23

Table 3.7 Acid digestion recovery (%) of CFA left in reservoir after PM standard preparation with the modified reservoir cassette (20 samples)

Mass (mg)	Mn	Ni	Cu	Zn	Pb
222.23	37.68	33.10	41.62	47.58	42.31
216.63	38.06	32.39	40.18	46.33	41.03
215.57	39.78	33.40	39.84	46.31	41.03
210.36	39.16	32.23	39.94	47.59	40.65
210.22	39.65	32.41	39.44	45.27	40.05
204.74	40.20	32.41	39.76	38.53	40.30
199.69	39.73	32.58	40.56	42.15	41.76
197.89	40.21	35.73	43.04	42.48	43.25
196.44	38.32	34.16	41.26	44.97	41.67
195.74	38.17	32.61	42.70	42.04	40.20
192.41	36.98	34.08	40.07	42.30	40.79
187.66	38.76	34.65	41.30	49.14	42.13
183.93	38.51	33.91	40.69	48.04	41.63
182.56	39.51	32.92	40.32	48.18	41.54
180.96	39.19	34.86	42.07	42.59	42.11
168.36	36.35	30.96	37.87	36.57	40.36
160.96	39.60	33.91	39.59	39.94	43.84
101.54	40.03	35.61	41.02	41.11	40.00
78.18	38.97	34.12	37.28	40.30	41.56
74.47	40.68	35.82	38.82	44.47	41.48

3.3 The Homogeneity of the PM Standards

The homogeneity of the SRM CFA 1633b on the PM standard was investigated using the method described in section 2.5. The evaluation of the results is addressed below.

3.3.1 Trace Elements Homogeneity

Laser ablation ICP-MS was used for the trace element homogeneity investigation. The time-resolved MS profiles of five analytes on one raster are shown as figure 3.2. Seven raster patterns of one PM standard were analyzed as described in Section 2.5.1. The regions of interest can be altered for individual samples post-run. For each region the average CPS per time slice is calculated.

The RSDs for the integrated signals of seven raster patterns for the five interested analytes (Mn, Ni, Cu, Zn, Pb) were calculated and listed in Table 3.8. The RSDs are 8% - 10%. The precision of the LA-ICP-MS signal is affected by many factors as described in Section 1.3.6. The variation of the operating conditions, such as beam homogeneity, power density, pulse width, focus position, causes 5% or even greater RSD, and the RSD for ICP-MS itself is about 2%. Therefore 8% - 10% RSD is an acceptable error.[51] These RSD values indicated that the PM on the filter is homogeneously distributed. The SRM NIST 614 glass standard was also analyzed to compare the RSDs with the PM standard. Table 3.9 presents the integrated signal and RSD for Nickle614. The RSDs of different elements for NIST 614 at about 10% are even greater than that of the PM standards, even though SRM NIST 614 is a recognized homogeneous reference standard. This result further confirmed that the RSDs for PM standard are mainly due to the instrument system, mostly the operation of the LA system.

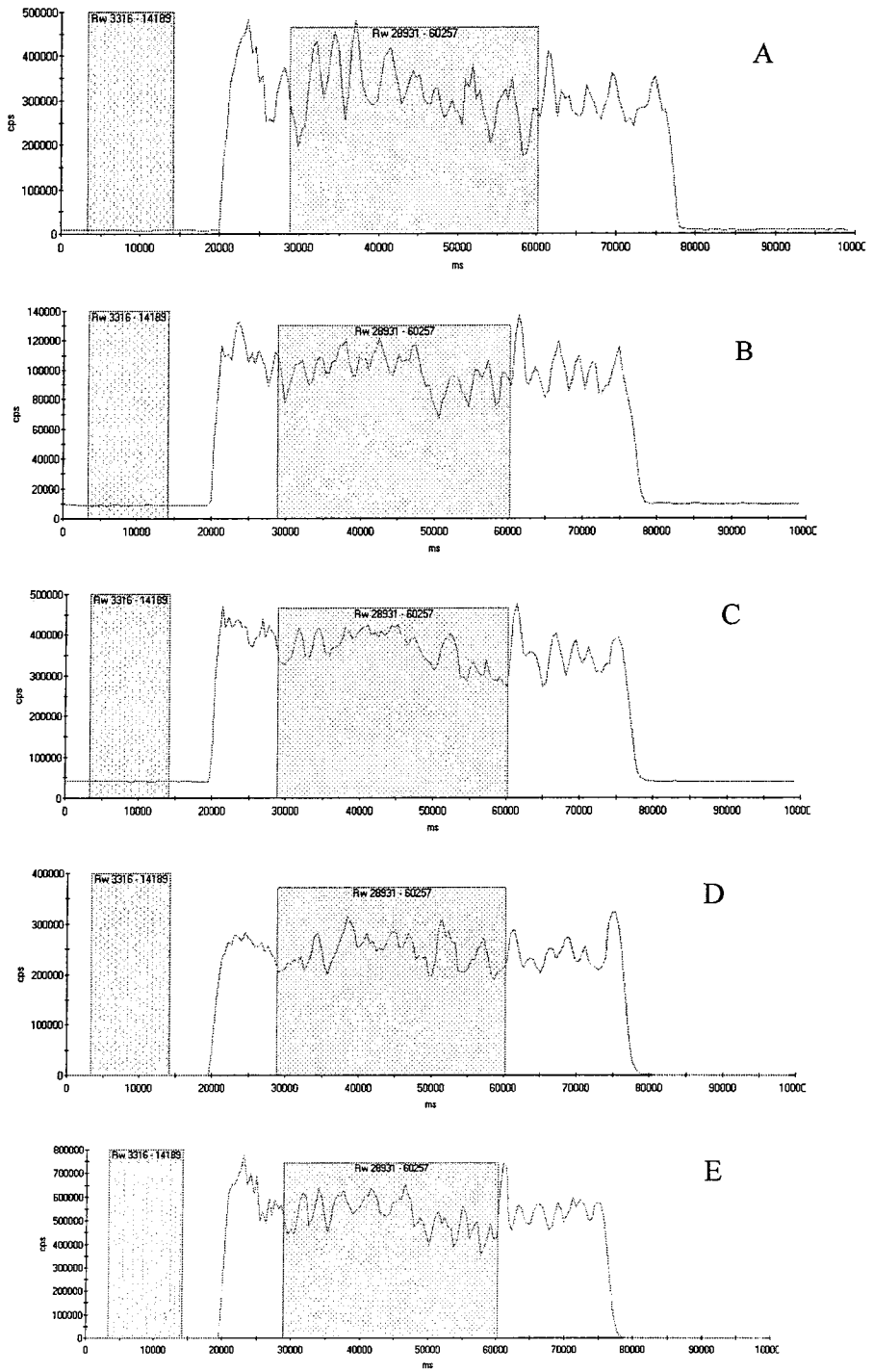

Figure 3.2 LA-ICP-MS transient signal for (A) Mn; (B) Ni, (C) Cu; (D) Zn; (E) Pb of one raster on one PM standard

Table 3.8 LA-ICP-MS signal and RSDs for a PM standard (9.37 mg)

Sample label	Integrated Signal (CPS)				
	55Mn	60Ni	63Cu	66Zn	208Pb
Raster 1	299139	100826	344390	231917	558304
Raster 2	328741	97901	359015	248345	538488
Raster 3	380185	111083	427182	254854	641032
Raster 4	331218	105241	410977	242599	560370
Raster 5	315630	98344	363145	244667	520203
Raster 6	340396	112828	406497	261952	614649
Raster 7	298746	89966	332676	211806	607600
Average	327722	102313	377697	242306	577235
STD	28074	8020	36703	16451	44326
RSD (%)	8.6	7.8	9.7	6.8	7.7

Table 3.9 LA-ICP-MS signal and RSDs for NIST 614

Sample lable	Integrated Signal (CPS)				
	55Mn	60Ni	63Cu	66Zn	208Pb
Raster 1	36169	19213	158018	37271	94063
Raster 2	43813	25194	175477	37880	85384
Raster 3	45360	25972	191744	35890	88217
Raster 4	39539	23366	158555	32010	81574
Raster 5	38484	21971	146257	30190	76389
Raster 6	38758	21644	145248	32170	74821
Raster 7	37992	21019	137781	28709	72405
Average	40016	22626	159012	33446	81836
STD	3317	2379	18914	3582	7860
RSD (%)	8.3	10.5	11.9	10.7	9.6

A series of six PM standards and a blank were prepared and analyzed by LA-ICP-MS. The calibration curves (Figure 3.3) for Mn, Ni, Cu, Zn, Pb were constructed according to the integrated signal (cps) and mass (ng) of each element. The coefficients of determination ranging from between 0.9626 for Zn to 0.9929 for Cu, were significantly improved compared with previous values that ranged from 0.8891 to 0.9707.[41] A better coefficient of determination indicated for the most part that the PM distribution on the filter was more homogeneous. The calibration curve with a better R^2 value is not only evidence of a homogeneous distribution of the PM on the filter, it also provides reliable analytical results for unknown sample analysis.

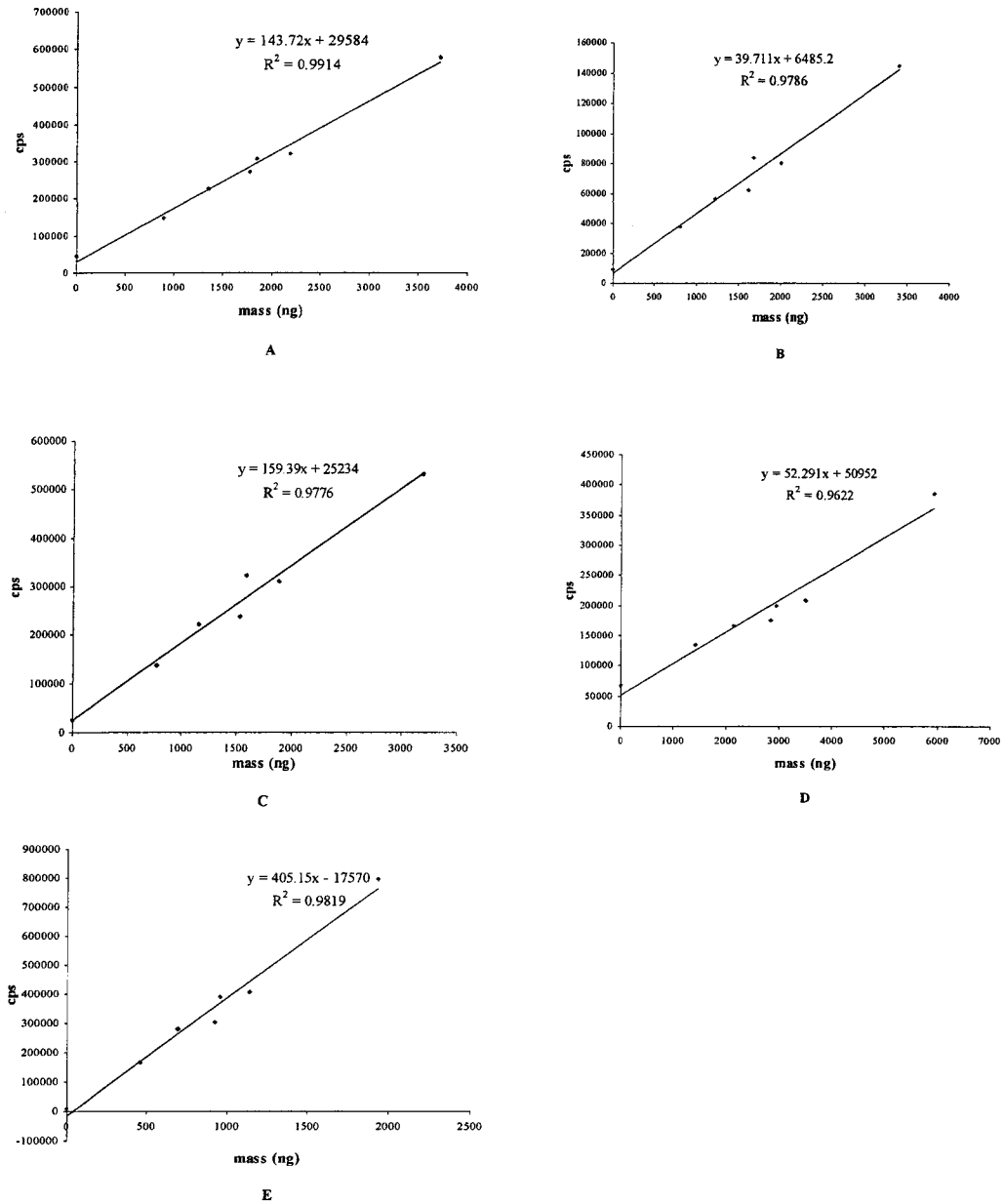

Figure 3.3 Calibration curves for **(A)** Mn; **(B)** Ni; **(C)** Cu; **(D)** Zn; **(E)** Pb

The mass of these standards and their preparation condition are presented in Table 3.10. The certified values of the interest metals are shown in Table 3.11. The mass of an element of one PM standard is calculated using the following equation:

Mass of element (ng) = certified value (ng/mg) × mass of filter standard (mg)

Table 3.10 Mass of filter standards and preparation condition

Standards	Mass (mg)	Flow rate×Application time×Applications
1	6.80	25×5×2
2	10.22	25×5×3
3	13.50	28×5×3
4	14.03	28×5×3
5	16.65	28×5×4
6	28.24	28×5×5

Table 3.11 NIST certified values for CFA 1633b

Element	Concentration (mg/kg)
Mn	131.8
Ni	120.6
Cu	112.8
Zn	210*
Pb	68.2

* Zn is a noncertified value

3.3.2 Major Elements Homogeneity

As introduced in chapter 2 section 2.5.2, SEM-EDS was used to investigate the major elements distribution of the PM on the filter. The PM standard SEM mappings for element Fe, P, Ti are shown as examples as Figure 3.4. It can be seen that the elements (lighter color or white dots) were homogeneously distributed on the filter. The percent normality for major elements Si, O, Al, Fe, Ca, K, and Ti of seven images on a 21.28 mg

PM standard were calculated as table 3.12. The RSDs, ranged from 1% to 5%, for the major elements (percent normality $\geq$ 1%) of Si, O, Al, Fe, Ca, K, and Ti, were small enough to indicate that the PM standard was homogeneous. The higher RSDs for minor elements of Na, Mg, S, and P were due mainly to the low concentration and the limit of detection of SEM-EDS as explained in chapter 2 section 2.5.2.

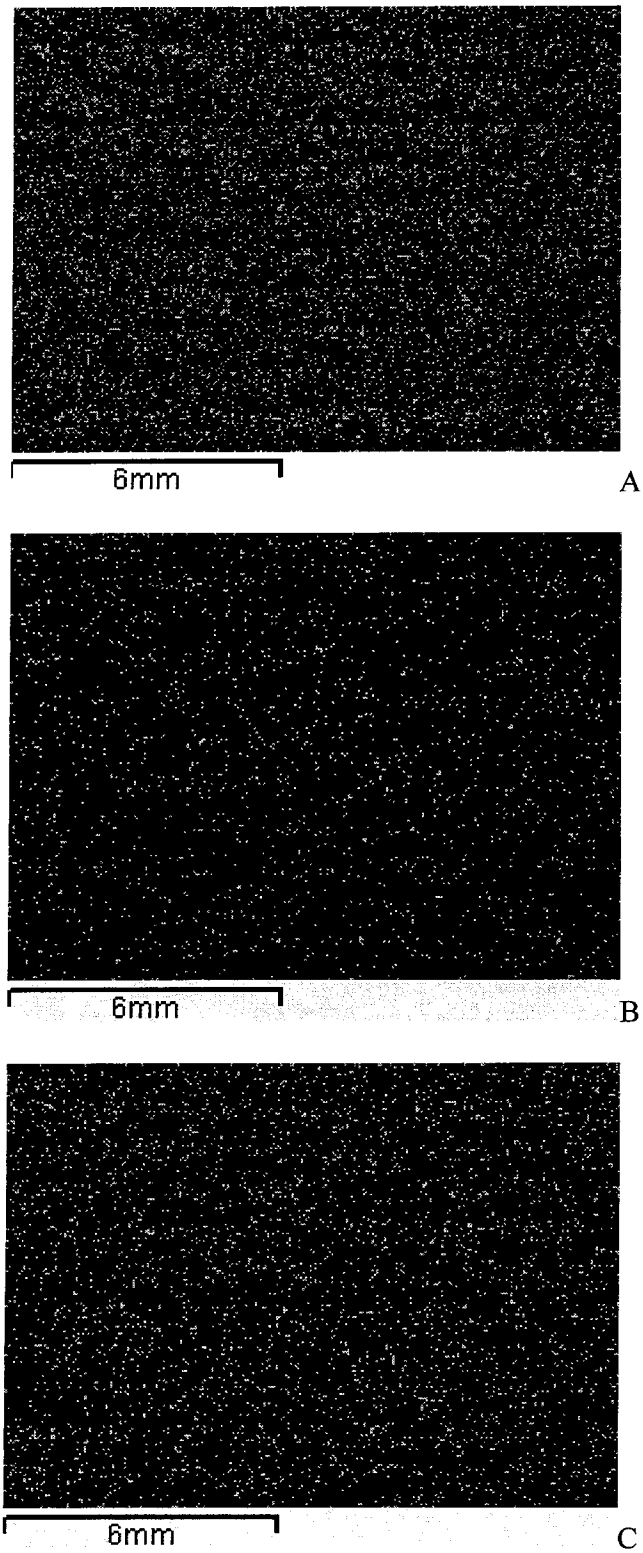

Figure 3.4 SEM-EDS maps of a 21.28 mg PMstandard for **(A)** Fe;**(B)** P;**(C)** Ti

Table 3.12 Si, O, Al, Fe, Ca, K, Ti relative concentrations of seven images of one 21.28 mg PM standard

	Si	O	Al	Fe	Ca	K	Ti	Na	Mg	S	P
Image 1	37.34	24.21	20.14	8.01	3.26	3.45	1.73	0.68	0.57	0.34	0.27
Image 2	37.74	24.36	20.14	7.73	3.31	3.30	1.58	0.63	0.63	0.34	0.25
Image 3	38.17	24.13	19.86	7.65	3.30	3.38	1.61	0.78	0.54	0.31	0.28
Image 4	38.37	23.87	19.59	7.61	3.58	3.33	1.60	0.86	0.61	0.31	0.28
Image 5	38.26	24.04	19.75	7.77	3.48	3.31	1.53	0.74	0.56	0.32	0.26
Image 6	37.76	24.69	19.75	7.47	3.48	3.29	1.57	0.75	0.61	0.28	0.34
Image 7	37.65	25.31	19.37	7.36	3.50	3.19	1.46	0.88	0.69	0.35	0.23
Average	37.90	24.37	19.80	7.66	3.42	3.32	1.58	0.76	0.60	0.32	0.27
S.D.	0.38	0.49	0.28	0.21	0.12	0.08	0.08	0.09	0.05	0.02	0.03
RSD (%)	0.99	2.00	1.41	2.76	3.61	2.42	5.21	11.84	8.39	7.50	12.65

3.4 Internal Standardization

Internal standards are essential for precise analyses because they allow correction for the variation caused by instrument drift or matrix effect. Ideally, internal standards should be non-interfered, mono-isotopic species. Commonly used internal standards include ^{9}Be, ^{45}Sc, ^{89}Y, ^{103}Rh, ^{115}In and ^{209}Bi. The internal standard element chosen should not be present in the samples and should be added to all blanks, standards and samples in equal concentrations. The behaviour of elements in Ar plasma is largely dependent on physical properties such as atomic mass and ionization efficiency. In order to correct effectively for temporal variations in signal intensity (largely dependent on

variations in the physical behavior of the analytes in the plasma), the physical properties of the internal standards must be carefully matched to those of the isotopes they are applied to (i.e. internal standards should have similar mass and ionization efficiency as the elements to which they are applied)[52]. For example, ^{103}Rh may be an appropriate internal standard for ^{85}Rb, ^{88}Sr, and ^{89}Y, while ^{209}Bi may work better for ^{208}Pb, ^{232}Th, and ^{238}U.

The certificate of the SRM CFA 1633b shows that Sc is present in CFA 1633b; therefore it is not suitable as an internal standard for this sample. The certificate does not indicate that Y is present, however, preliminary studies using SN-ICP-MS showed that Y was present in sufficient amount to disqualify it as suitable internal standard. Therefore, in order to cover the whole mass range of the analytes, Be, In, and Bi were chosen as internal standards for SN-ICP-MS analysis of the acid digested samples. The results showed these internal standards worked well. This meant the ionization efficiency of the ICP was almost the same during the whole run and the sample matrix did not seriously affect the instrument performance.

It was proposed by Samson[41] that adding internal standards in the PVAc coating may correct the variation in the analyte response due to the variation in the polymer coating thickness and also correct for any variation in the instrument response due to instrument drift. A better linear relationship should be obtained between the analytical signal and the analyte (i.e. target element) mass/concentration. Therefore internal standardization technique was investigated by adding internal standards into the PVAc solution and spraying them onto the PM standards.

However, the expected result was not achieved even after several trials. From the viewpoint of theory, only if the signal of the analyte and of the internal standard is equally affected by the variation of the coating thickness, the ratio of the analyte signal to the internal standard signal would be independent of the coating thickness variation, and the internal standardization technique would compensate for the coating thickness variation and instrument drift. Alternatively, if the internal standards are homogeneously distributed on the PM standard, it should correct the instrument drift. However, the analyte and the internal standard were deposited onto the filter during two different operations. The analyte was applied onto the filter by PM standard preparation procedure using the apparatus developed in current study, whereas the internal standards were sprayed onto the PM standards during the PVAc coating process. An absolutely homogeneous PVAc coating or internal standard deposition could not be obtained due to the limitations in the spray technique. Therefore the instrument drift could not be corrected by internal standards applied in this way. It was also impossible to ensure that the spot which has thicker/thinner PVAc coating, i.e, more/less internal standard, had received more/less analyte in the PM standard which is the only way that the internal standardization technique corrects for the effects of the varying thickness of the PVAc coating. As figure 3.5 shows, the signal of the analytes (Figure 3.5 A, B, C, D, E) did not follow the same trend with the internal standard signal (Figure 3.5 F). For example, there was no big drift at 20000 ms ~ 70000 ms period and there was a signal drop around 75000 ms, which meant that probably less PM was deposited at that point, for all the analyte signals. However, two big peaks between 2000 ms and 70000 ms were observed for the internal standard signal and no obvious signal drop was seen at 75000 ms on the

internal standard (In) signal curve. Therefore this internal standardization method could not correct for the coating thickness variation and instrument drift.

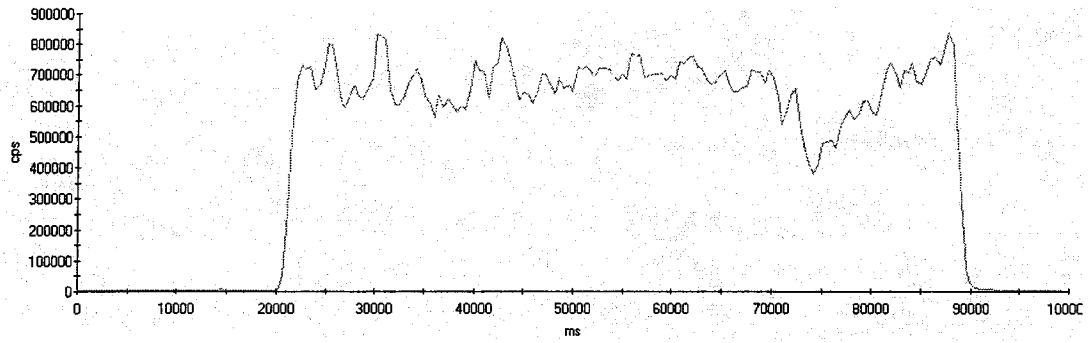

A

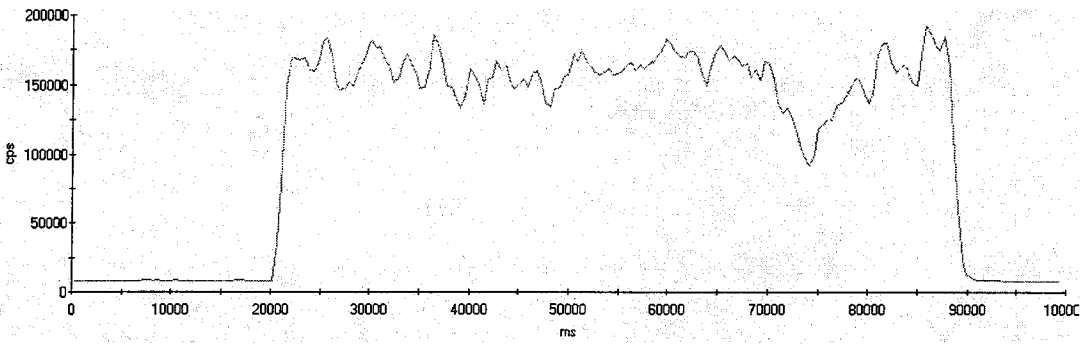

B

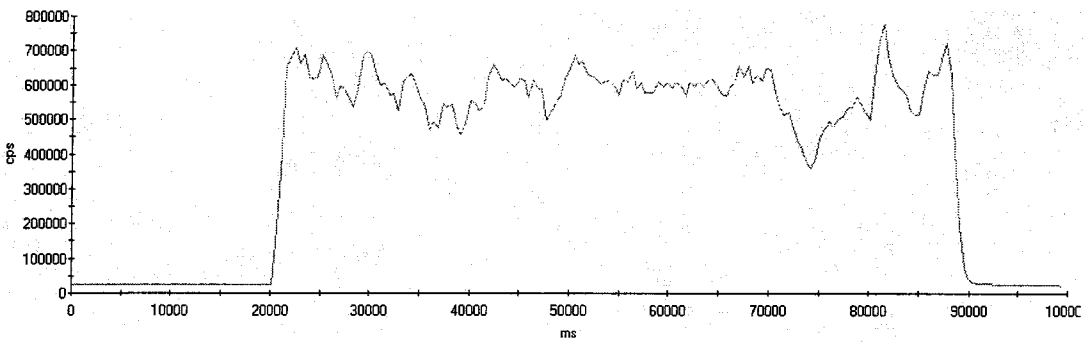

C

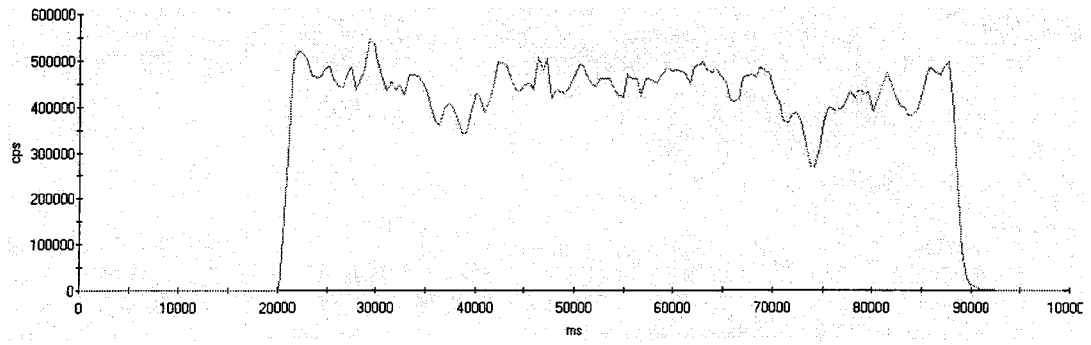

D

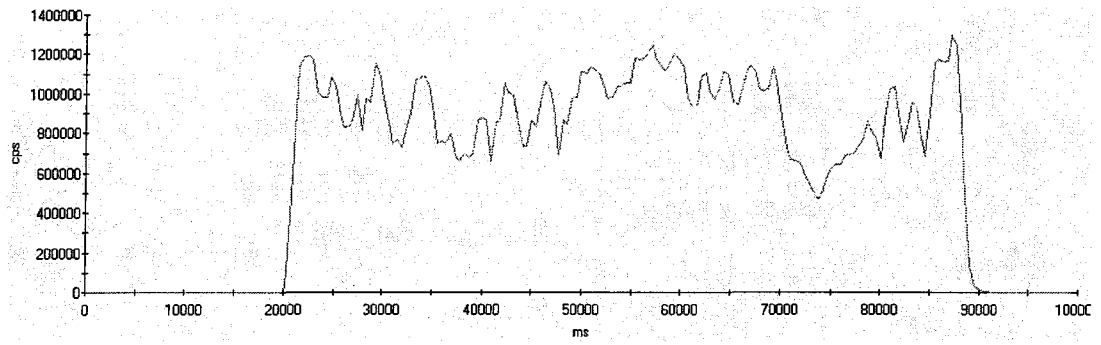

E

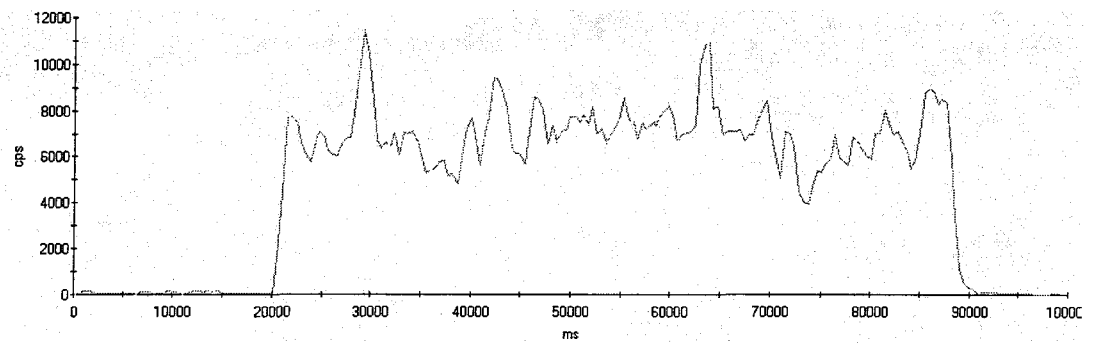

F

Figure 3.5 LA-ICP-MS transit signal for analytes (A) Mn; (B) Ni; (C) Cu; (D) Zn; (E) Pb; and internal standard (F) In of a 28.24 mg PM standard.

3.5 Poly(vinyl acetate) (PVAc) Coating

The polyvinyl acetate (PVAc) coating has dual advantages, pointed out by Samson[41], of protecting the PM on the filter and aiding in the laser ablation process from the ablation track. However, the influence of the PVAc coating on the LA-ICP-MS signal should be investigated. Therefore a number of filter blanks with 0.1 M PVAc coating and filter blanks without PVAc coating were analyzed by LA-ICP-MS. This investigation was done at different mass spectrometer dwell times (10 ms, 50 ms, 100 ms, and 250 ms). The concentration of Ni and Cu in the filter blank was too low to be measured by LA-ICP-MS. Therefore only Mn, Zn, and Pb signals were recorded and calculated as figure 3.6. The PVAc coating increased the Mn signal at any dwell time but the Mn signal was increased more at the 10 ms dwell time than at longer dwell times. At the 100 ms dwell time, the Mn signal was increased 34.0%. The Zn signal was increased by the PVAc coating at 10 ms dwell time, however, it was decreased by the PVAc coating at longer than 50ms dwell times, for example, the Zn signal was decreased by 19.8% at the 100 ms dwell time. The Pb signal was increased by the PVAc coating at longer than 50 ms dwell times but the uncoated filter generated a higher signal intensity at the 10 ms dwell time. For example, a 12.6% signal increase was obtained for Pb at the 100 ms dwell time. Thus no clear conclusion can be drawn at this point.

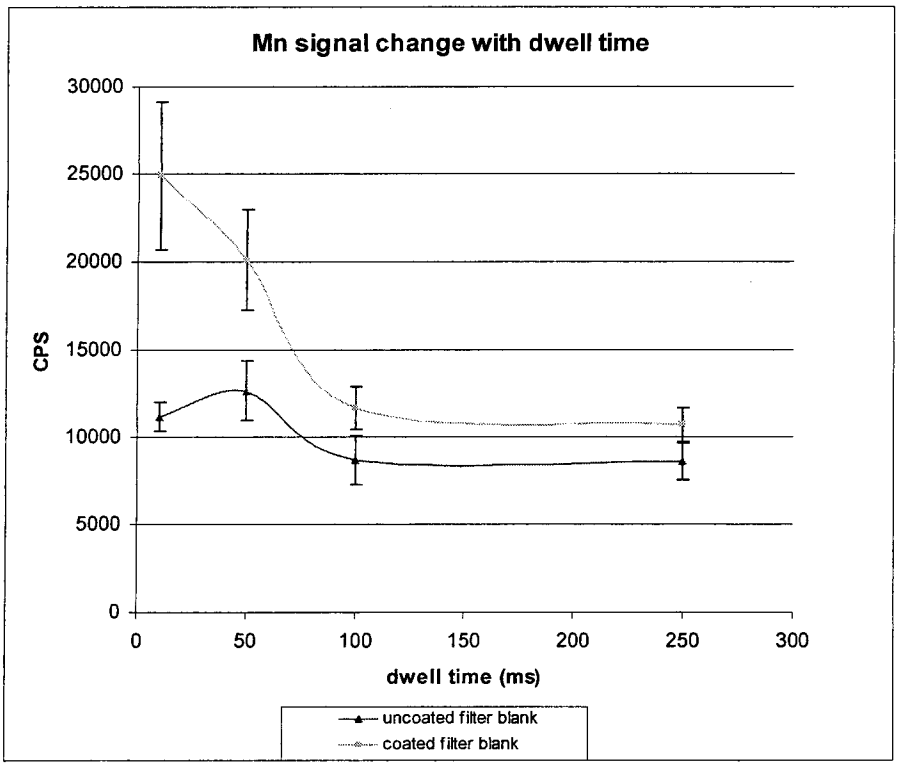

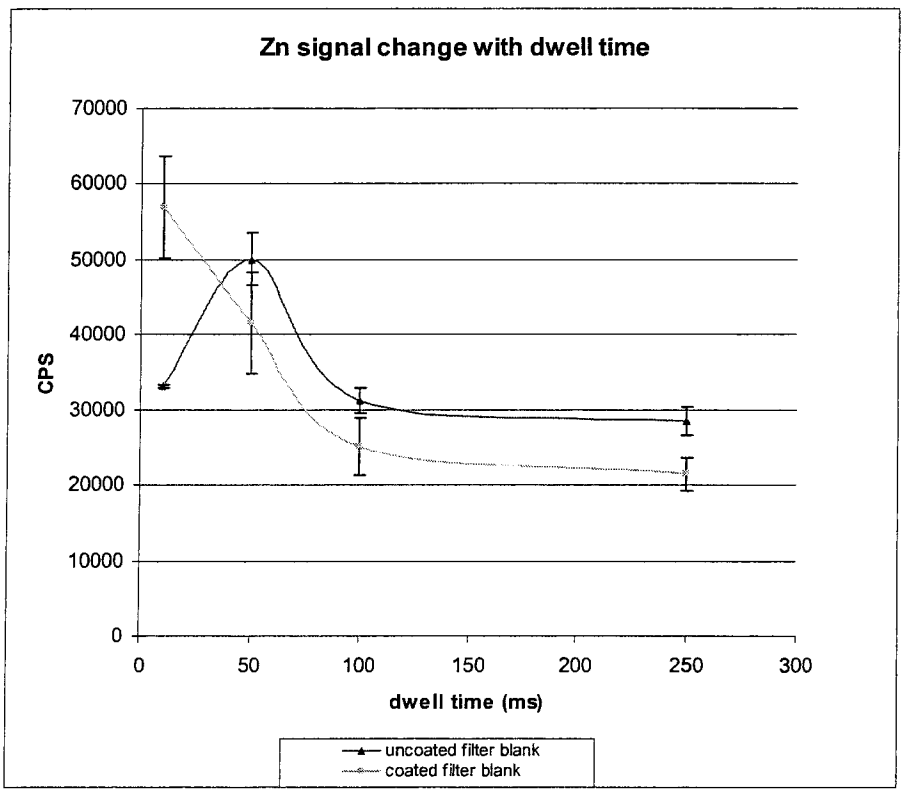

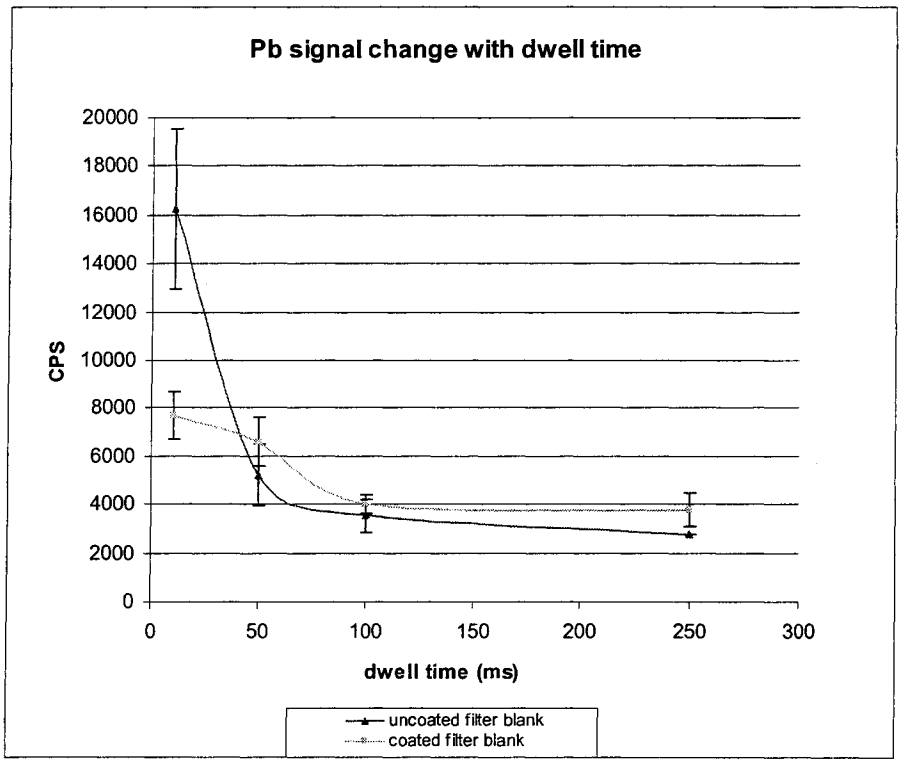

Figure 3.6 Coated /uncoated filter blank signal *vs* dwell time

3.6 The Helium effect

Because of the benefit of helium as an ablation/carrier gas, helium was connected to the laser ablation unit and used as ablation and carrier gas in this study. The configuration of the connection is shown in Figure 2.6. A comparison of He and Ar as ablation/carrier gases was done with NIST 614 glass standard. The results are shown as table 3.13. The signal intensity of Ni was increased 25.4%, the strontium (Sr) signal was increased 12.3%, and the U signal was increased 15.2% by using He as the ablation gas. Pb did not show any increase, a 4.1% decrease was observed instead. However, 4.1% is within the range of the ≤ 10% error associated with LA-ICP-MS analysis as discussed in 3.3.1. Thus, the observed 4.1% decrease may not be caused by the use of helium as the

ablation gas. Therefore helium was used as the ablation/carrier gas for LA-ICP-MS analysis in the current study.

Table 3.13 Comparison of signal intensity of NIST 614 using He/Ar as ablation gas

	Ni	Sr	Pb	U
Ar	108847	536287	1207703	476608
He	136445	602490	1158187	549052
% of increase	25.4	12.3	-4.1	15.2

Summary and Conclusions

An apparatus for preparing PM standards has been developed by investigating the performance of the main components of the apparatus, the drift tube and the reservoir cassette. The PM standard, prepared using SRM CFA 1633b, was used as the test sample for the developed apparatus and a combination of instrument analysis techniques were employed to evaluate the performance of the apparatus by determining the homogeneity and chemical integrity of the PM standards.

The PM standards were coated with PVAc/MeOH solution using a spray technique for LA-ICP-MS analysis. The effect of the PVAc coating on the LA-ICP-MS signal of the PM standard was investigated in a preliminarily study. No clear conclusion could be drawn because the various effects were obtained for different analytes at different mass analyzer dwell times.

Helium was chosen as the ablation gas for LA-ICP-MS analysis of PM standards. A preliminary investigation comparing the LA-ICP-MS signal intensity between the helium and argon was done using SRM 614 as the sample. It was found that the signal intensity can be improved by using helium, by about 10% - 25%. The exception was for Pb.

Solution nebulization ICP-MS analysis of acid digested CFA 1633b was used to investigate the chemical integrity of the PM standard and a suitable acid digestion method was evaluated. The ANOVA analysis of the acid digestion recovery indicated that the chemical integrity of the CFA 1633b is preserved after the PM standard preparation process using the developed apparatus in this study.

Scanning electron microscope-energy dispersive X-ray spectroscopy was used to investigate the major element distribution in the PM standards by providing elemental

distribution maps of the PM on the filter. It was concluded that the PM was homogeneously distributed on the filter.

Laser ablation ICP-MS analysis was also used to evaluate the homogeneity of the PM standard by analyzing for trace elements. The relative standard deviation of the LA-ICP-MS signal intensity for the five metals of interest from seven raster sites was comparable with the homogeneous SRM 614 glass standard. The calibration curves of the interest analytes (Mn, Ni, Cu, Zn, and Pb) in CFA 1633b filter standards, prepared using the developed apparatus, were constructed based on the LA-ICP-MS analysis and the R^2 values of the calibration curves ranged from 0.9622 for Zn to 0.9914 for Mn. Both SEM-EDS and LA-ICP-MS analyses provided evidence that the PM was homogeneously distributed on the filter.

Suggestions for future work

The apparatus developed in the present study is for the preparation of calibration standards that can be used for the direct analysis of solid environmental samples. Using standard reference material CFA 1633b as the test sample, the apparatus was shown to be successful. However, its application should be tested with other environmental samples such as sediments as the complexity of the matrix is always a challenge on environmental samples. One type of sediment SRM Hiss-1 was tried using the developed apparatus. However, the physical characteristic differences (the density and the particulate diameter, the particulate surface property) revealed more difficulty with preparing Hiss-1 standards than CFA 1633b standards. The Hiss-1 was difficult to transfer and easily fall off the filter. Therefore, further modifications may be needed; a higher flow rate may be required, and polymer coating may need to be applied on the blank filter before the PM standard preparation to keep the PM on the filter.

Internal standardization is an important and efficient technique for the correction of matrix effects and instrument drift for LA-ICP-MS analysis. The method tried in current study not successful. A major element such as Si in the SRM may be used as internal standard. This could be rapidly determined by XRF without destroying the PM standards. A reproducible signal for Si can be obtained with the normalization of the XRF measurement, and thus be utilized as a naturally occurring internal standard.

The acid digestion method used in this study is not a total digestion method. Limitation of facilities prevented the use of a total digestion method. A total acid

digestion method could be used to investigate the chemical composition of the PM standard. Particle size may affect the acid digestion recovery if it is not a total digestion, whereas it may or may not affect the LA-ICP-MS analysis. However, the impact the particle size on laser ablation should be investigated in that case.

A preliminary investigation was done for the impact of the PVAc coating on the PM standard, and the impact of helium as ablation gas on LA-ICP-MS signal. However, the data were not sufficient to support a clear conclusion. A more extensive investigation should be performed. Such as the pictures of LA image could be taken to compare the difference between Ar and He as ablation gases. Different materials could be used as the LA samples to investigate the effect of He as the ablation gas.

The purpose of calibration standards is to establish the relation between the analytical signal and the concentration/mass of the sample. Thus the unknown sample from the real world can be analyzed based on the calibration curve. Therefore an application, i.e., analysis of real samples collected from around an industrial emission should be done to further test if the PM standards prepared using the developed apparatus in current study can be used for monitoring environmental problems in Canada or elsewhere.

The development of the apparatus in this thesis research for improved PM distribution homogeneity is a useful practical contribution to the analysis of airborne particulate matter using laser ablation-inductively coupled plasma-mass spectrometry.

References

1 *The Particle Pollution Report: Current Understanding of Air Quality and Emissions through 2003:* December 2004; EPA 454-R-04-002; U.S. Environmental Protection Agency; Office of Air Quality Planning and Standards Emissions, Monitoring, and Analysis Division Research Triangle Park, North Carolina, USA.

2 *Basic Environmental Toxicolog;* Cockerham, Lorris G. and Shane, Barbara S., Eds.; CRC Press: Boca Raton, USA, 1994.

3 http://www.digitalnaturopath.com (July, 2005).

4 Hughes, W. W.; *Essentials of Environmental Toxicology: The Effects of Environmentally Hazardous Substances on Human Health*; Taylor and Francis Publishers: Levittown, PA, USA, 1996.

5 Joselow, M. M., Tobias, E., Koehler, R., Coleman, S., Bogden, J., and Gause, D. *Amer. J. Public Health*, **1978**, *68*, (6) p. 557.

6 *Medical and biological effects of environmental pollutants – Nickel. Committee on Medical and Biological Effects of Environmental Pollutants:* 1975; National Research Council; National Academy Press, Washington, DC, USA.

7 Jacobs, M. B.; *The Analytical Toxicology of Industrial Inorganic Poisons.* Interscience Publishers: 1967.

8 Newman, M. C.; *Fundamentals of Ecotoxicology.* Ann Arbor Press: 1998.

9 Waldron, H. A.; *Metals in the Environment.* Academic Press: 1980.

10 http://www.incowatch.ca (July, 2005).

11 http://www.aep.com (July, 2005).

12 *Medical and biological effects of environmental pollutants – Copper. Committee on Medical and Biological Effects of Environmental Pollutants:* 1977; National Research Council. National Academy Press, Washington, DC, USA.

13 Luckey, et. al, *Environmental Quality and Safety, Heavy Metal Toxicity Safety and Hormology.* Georg Thieme Publisher: 1975, p4.

14 http://www.freedrinkingwater.com (July, 2005).

15 http://www.diagnose-me.com (July, 2005).

16 http://www.ecoonespa.com (July, 2005).

17 http://www.atsdr.cdc.gov (July, 2005).

18 Houk, R. S., Fassel, V. A., Flesch, G. D., Svec, H. J., Gray, A. L. and Taylor, C. E.; *Analytical Chemistry* **1980**, *52*, 2283.

19 Gray, A. L.; *The Analyst* **1985**, *110*, 551.

20 Taylor, H. E.; *Inductively Coupled Plasma Mass Spectrometry: Practices and Techniques;* Academic Press: San Diego, USA, 2001.

21 Hill, S. J.; *Inductively Coupled Plasma Mass Spectrometry and its Applications*; CRC Press: Boca Raton, USA, 1999; 119, pp35-37.

22 Skoog, D. A., Holler, F. J., and Nieman, T. A., *Principles of Instrumental Analysis 5th Edn.;* Harcourt Brace College Publishers: 1998.

23 Thomas, R.; A Beginner's Guide to ICP-MS. *Spectroscopy* [Online] **2001**, *16* (6).

24 Ohata, M., Yasuda, H., Namai, Y., and Furuta, N. *Anal. Sci.* **2002**, *18*, 1105.

25 Tibi, M. and Heumann, K. G

26 Boue-Bigne, F., Masters, B. J., Crighton, J. S. and Sharp, B. L. . *J. Anal. At. Spectrom.* **1999**, *14*, 1665.

27 Günther, D., Frischknecht, R., Muschenborn, H. J., Heinrich, C. A. *Fresenius Journal of Analytical Chemistry* **1997**, *359*, 390.

28 Masters, B. J. and Sharp, B. L. *Anal. Comm.* **1997**, *34*, 237.

29 Aeschliman, D. B., Bajic, S. J., Baldwin, D. P. and Houk, R. S. *J. Anal. At. Spectrom.* **2003**, *18*, 872.

30 Leach, J. J., Allen L. A., Aeschliman, D. B., Houk, R. S. *Anal. Chem.* **1999**, *71*, 440.

31 Bellotto, V. R. and Miekeley, N. *Fresenius Journal of Analytical Chemistry* **2000**, *367*, 635.

32 Chin, C., Wang, C. and Jeng, S. *J. Anal. At. Spectrom.* **1999**, *14*, 663.

33 Ødegård, M., Mansfeld, J., Dundas, S. H. *Fresenius Journal of Analytical Chemistry*, 2001, *370*, 819.

34 Pickhardt, C. and Becker, J. S. *Fresenius Journal of Analytical Chemistry,* **2001**, *370*, 534.

35 Raith, A., Godfrey, J., Hutton, R. C., *Fresenius Journal of Analytical Chemistry,* **1996**, *354*, 163.

36 Günther, D., Quadt, A. v., Wirz, R., Cousin, H. and Dietrich, V. J. *Mikrochim. Acta*, **2001**, *136*, 101.

37 Tanaka, S., Yasushi, N., Sato, N., Fukasawa, T., Santosa, S. J., Yamanaka, K., and Ootoshi, T. *J. Anal. At. Spectrom.* **1998**, *13*, 135.

38 Wang, C., Jeng, S., Lin, C. C., Chiang, P. *Anal. Chim. Acta,* **1998**, *368*, 11.

39 Chin, C., Wang, C., and Jeng, S. *J. Anal. At. Spectrom.* **1999**, *14*, 663.

40 Wang, C., Chin, C., Luo, S., Men, L., *Anal. Chim. Acta.* **1999**, *389*, 257.

41 Samson, J. Method Development for the Preparation of Calibration Standards for Laser-Ablation Inductively Coupled Plasma-Mass Spectrometry. Honors Thesis, Saint Mary's University, Halifax, NS, Canada, May, 2003.

42 Acid digestion of sediments, sludges, and soils. http://www.epa.gov/epaoswer/hazwaste/test/pdfs/3050b.pdf Environment Protection Agency: 1996.

43 Jeffries, T. E., Perkins, W. T. and Pearce, N. J. G. *The Analyst*, **1995**, *120*, 1365.

44 Motelica-Heino M, Donard O. F. X., Mermet J.M. *J. Anal. At. Spectrom.* **1999**, *4*, 675.

45 Günther, D. and Heinrich, C. A.. **1999**, *14*, 1369.

46 Mank, A. J. G. and Mason, P. R. D. *J. Anal. At. Spectrom.* **1999**, *14*, 1143.

47 Russo, R. E., Mao, X. L., Borisov, O. V. and Liu, H. . *J. Anal. At. Spectrom.* **2000**, *15*, 1115.

48 Eggins, S. M., Kinsley, L.P.J., and Shelley, J. M. G. *Appl. Surf. Sci.* **1998**, *129*, 278.

49 Guillong, M. and Günther, D. . *J. Anal. At. Spectrom* **2002**, *17*, 831.

50 Skoog, D.; West, D.; Holler, J.; and Crouch, S.; Statistical Data Evaluation and Treatment. *Fundamentals of Analytical Chemistry, 8th Edn;* Brooks/Cole-Thomson Learning: Belmont, California, USA, 2004.

51 Durrant, S. F. and Ward, N. I. . *J. Anal. At. Spectrom.* **2005**, *20*, 821.

52 Rodushkin, I., Axelsson, M. D., Malinovsky, D. and Baxter, D. C. *J. Anal. At. Spectrom.* **2002**, *17*. 1231.

Appendices

Appendix 1. Recovery comparison of different amount concentrated nitric acid used for acid digestion.

Hypothesis: There are no significant differences, at 95% confidence level, between the acid digestion recoveries when different amount (10mL, 15mL, 20mL) HNO_3 was used to digest 0.25g SRM CFA 1633b sample.

Procedure: A number of representative amounts of 0.25g CFA 1633b samples were digested following the digestion procedure described in section 2.4.1. The only difference for the three different experiments was the amount of concentrated HNO_3 added to the sample when doing the acid digestion. The recovery for each sample was calculated based on the SN-ICP-MS analysis data and the certified value of the SRM.

ANOVA analysis: ANOVA analysis was done using Microsoft Excell Spreadsheet. If $F_{calculated} < F_{critical}$ at 95% confidence level, the experimental means are identical, and the numerical difference is the result of the random errors inevitable in all measurements or the results of systematic errors.

Results: The calculation was done based on table 3.1, table 3.2, and table 3.3. The calculation for Ni was not done because the mistake of choosing the isotope as discussed in section 3.2.2.1. $F_{calculated} < F_{critical}$ for the other four analytes, therefore, there were no

statistical difference, at 95% confidence level, for the acid digestion recoveries when different amount concentrated HNO_3 used for acid digestion.

Mn recovery ANOVA

Anova: Single Factor

SUMMARY

Groups	*Count*	*Sum*	*Average*	*Variance*
10mL HNO3	3	109.02	36.34	2.1568
15mL HNO3	2	70.1	35.05	1.125
20mL HNO3	3	114.3	38.1	1.75

ANOVA

Source of Variation	*SS*	*df*	*MS*	*F*	*P-value*	*F crit*
Between Groups	11.70975	2	5.854875	3.275051	0.123299	5.786148
Within Groups	8.9386	5	1.78772			
Total	20.64835	7				

Cu recovery ANOVA

Anova: Single Factor

SUMMARY

Groups	*Count*	*Sum*	*Average*	*Variance*
10mL HNO3	3	99.5	33.16667	0.063333
15mL HNO3	2	63.1	31.55	0.605
20mL HNO3	3	102.2	34.06667	1.463333

ANOVA

Source of Variation	*SS*	*df*	*MS*	*F*	*P-value*	*F crit*
Between Groups	7.621667	2	3.810833	5.208428	0.059901	5.786148
Within Groups	3.658333	5	0.731667			
Total	11.28	7				

Zn recovery ANOVA

Anova: Single Factor

SUMMARY

Groups	*Count*	*Sum*	*Average*	*Variance*
10mL HNO3	3	114.2	38.06667	25.52333
15mL HNO3	2	66.9	33.45	1.125
20mL HNO3	3	108	36	1.99

ANOVA

Source of Variation	*SS*	*df*	*MS*	*F*	*P-value*	*F crit*
Between Groups	25.66708	2	12.83354	1.142757	0.390189	5.786148
Within Groups	56.15167	5	11.23033			
Total	81.81875	7				

Pb recovery ANOVA

Anova: Single Factor

SUMMARY

Groups	*Count*	*Sum*	*Average*	*Variance*
10mL HNO3	3	124.9	41.63333	0.013333
15mL HNO3	2	80.4	40.2	1.62
20mL HNO3	3	123.8	41.26667	3.903333

ANOVA

Source of Variation	*SS*	*df*	*MS*	*F*	*P-value*	*F crit*
Between Groups	2.545417	2	1.272708	0.673153	0.550963	5.786148
Within Groups	9.453333	5	1.890667			
Total	11.99875	7				

Appendix 2 Acid digestion recovery comparison of original CFA 1633b, CFA 1633b left in the reservoir after the first series of PM standards preparation, CFA 1633b left in the reservoir after the second series of PM standards preparation.

Hypothesis: There are no significant differences, at 95% confidence level, among the acid digestion recoveries of original CFA 1633b, CFA 1633b left in the reservoir cassette after the first series (experiment 1), and the second series (experiment 2) PM standard preparation.

Procedure: A number of representative amounts of 0.25g original CFA 1633b samples were digested following the digestion procedure described in section 2.4.1 and analyzed by SN-ICP-MS. Two series of nine and twenty PM standards were prepared using the developed apparatus in current study. The CFA 1633b left in the reservoir cassette was digested by concentrated nitric acid, and analyzed by SN-ICP-MS as experiment 1 and experiment 2 respectively. The recovery for each sample was calculated based on the SN-ICP-MS analysis data and the certified value of the SRM.

ANOVA analysis: ANOVA analysis was done using Microsoft Excell Spreadsheet. If $F_{calculated} < F_{critical}$ at 95% confidence level, the experimental means are identical, and the numerical difference is the result of the random errors inevitable in all measurements or the results of systematic errors.

Results: The calculation was done based on table 3.5, table 3.6, and table 3.7. $F_{calculated} < F_{critical}$ for Mn, Cu, and Pb when the recoveries of original sample, experiment 1 sample, and experiment 2 sample were compared. Ni recovery of experiment 1 was different from the original and experiment 2. The possible reason was explained in chapter 3 section 3.2.2.2. $F_{calculated} > F_{critical}$ for Zn when three experimental means were compared. However, $F_{calculated} < F_{critical}$ when experiment 1 and experiment 2 compared with the original sample separately. Therefore we still can conclude that the PM standard preparation procedure did not change the chemical integrity of the original sample CFA 1633b.

Mn recovery comparison of original sample, experiment 1, and experiment 2

Anova: Single Factor

SUMMARY

Groups	*Count*	*Sum*	*Average*	*Variance*
Original	8	303.5365328	37.9420666	1.096221
Exp1	9	344.39	38.26555556	2.155478
Exp2	20	779.54	38.977	1.273748

ANOVA

Source of Variation	*SS*	*df*	*MS*	*F*	*P-value*	*F crit*
Between Groups	7.297729	2	3.648864396	2.525752	0.094907	3.2759
Within Groups	49.11859	34	1.444664469			
Total	56.41632	36				

Ni recovery comparison of original sample, experiment 1, and experiment 2

Anova: Single Factor

SUMMARY

Groups	*Count*	*Sum*	*Average*	*Variance*
original	8	260.0112	32.5014	1.884432
exp1	9	272.63	30.29222	0.982319
exp2	20	671.86	33.593	1.742991

ANOVA

Source of Variation	SS	df	MS	F	P-value	F crit
Between Groups	67.6533	2	33.82665	21.23283	1.04E-06	3.2759
Within Groups	54.1664	34	1.593129			
Total	121.8197	36				

Ni recovery comparison of original sample and experiment 1

Anova: Single Factor

SUMMARY

Groups	*Count*	*Sum*	*Average*	*Variance*
original	8	260.01119	32.5013989	1.884432405
exp1	9	272.63	30.2922222	0.982319444

ANOVA

Source of Variation	*SS*	*df*	*MS*	*F*	*P-value*	*F crit*
Between Groups	20.67019	1	20.6701898	14.72964359	0.001613	4.543068
Within Groups	21.04958	15	1.40330549			
Total	41.71977	16				

Ni recovery comparison of original sample and experiment 2

Anova: Single Factor

SUMMARY

Groups	*Count*	*Sum*	*Average*	*Variance*
original	8	260.0112	32.50139887	1.884432
exp2	20	671.86	33.593	1.742991

ANOVA

Source of Variation	*SS*	*df*	*MS*	*F*	*P-value*	*F crit*
Between Groups	6.809102989	1	6.809102989	3.823038	0.061381	4.2252
Within Groups	46.30784683	26	1.781071032			
Total	53.11694982	27				

Cu recovery comparison of original sample, experiment 1, and experiment 2

Anova: Single Factor

SUMMARY

Groups	*Count*	*Sum*	*Average*	*Variance*
original	8	325.7973129	40.724664	2.22127534
exp1	9	350.11	38.901111	5.24723611
exp2	20	807.37	40.3685	2.09835026

ANOVA

Source of Variation	*SS*	*df*	*MS*	*F*	*P-value*	*F crit*
Between Groups	17.49467	2	8.7473347	3.05362636	0.06030482	3.27590044
Within Groups	97.39547	34	2.8645727			
Total	114.8901	36				

Zn recovery comparison of original sample, experiment 1, and experiment 2

Anova: Single Factor

SUMMARY

Groups	*Count*	*Sum*	*Average*	*Variance*
original	8	342.28761	42.785951	12.528222
exp1	9	362.11	40.234444	5.4218278
exp2	20	875.89	43.7945	12.458805

ANOVA

Source of Variation	*SS*	*df*	*MS*	*F*	*P-value*	*F crit*
Between Groups	78.7243234	2	39.362162	3.6388032	0.0369824	3.27590044
Within Groups	367.789473	34	10.817337			
Total	446.513796	36				

Zn recovery comparison of original sample and experiment 1

Anova: Single Factor

SUMMARY

Groups	*Count*	*Sum*	*Average*	*Variance*
original	8	342.28761	42.785951	12.528222
exp1	9	362.11	40.234444	5.4218278

ANOVA

Source of Variation	*SS*	*df*	*MS*	*F*	*P-value*	*F crit*
Between Groups	27.5725606	1	27.572561	3.1554249	0.0959572	4.54306814
Within Groups	131.072178	15	8.7381452			
Total	158.644739	16				

Zn recovery comparison of original sample and experiment 2

Anova: Single Factor

SUMMARY

Groups	*Count*	*Sum*	*Average*	*Variance*
original	8	342.28761	42.785951	12.528222
exp2	20	875.89	43.7945	12.458805

ANOVA

Source of Variation	*SS*	*df*	*MS*	*F*	*P-value*	*F crit*
Between Groups	5.81240119	1	5.8124012	0.4658308	0.5009477	4.22519975
Within Groups	324.414851	26	12.477494			
Total	330.227252	27				

Pb recovery comparison of original sample, experiment 1, and experiment 2

Anova: Single Factor

SUMMARY

Groups	*Count*	*Sum*	*Average*	*Variance*
original	8	343.25278	42.9065969	4.51580122
exp1	9	372.44	41.3822222	7.57464444
exp2	20	827.69	41.3845	1.06662605

ANOVA

Source of Variation	*SS*	*df*	*MS*	*F*	*P-value*	*F crit*
Between Groups	14.5403596	2	7.2701798	2.19772447	0.12658605	3.2759004
Within Groups	112.473659	34	3.3080488			
Total	127.014019	36				